Journal of the Geological Society

High-energy flood events recorded in the Mesoproterozoic Meall Dearg Formation , NW Scotland; their recognition and implications for the study of pre-vegetation alluvium

--Manuscript Draft--

High-energy flood events recorded in the Mesoproterozoic Meall Dearg Formation, NW Scotland; their recognition and implications for the study of pre-vegetation alluvium

William J. McMahon*, Neil S. Davies

University of Cambridge, Department of Earth Sciences, Downing Street, Cambridge CB2 3EQ, United Kingdom

*wjm39@cam.ac.uk

ABSTRACT

The Mesoproterozoic-Neoproterozoic Torridonian Sandstone of NW Scotland has renewed sedimentological significance following recent advances in the understanding of pre-vegetation alluvium, as it is one of the most extensive and easily-accessible successions of such strata worldwide. This paper presents the first modern sedimentological analysis of the unit's constituent Meall Dearg Formation (late Mesoproterozoic), recognizing a dominance of alluvial facies, with subordinate aeolian facies. Alluvial strata within the Meall Dearg Formation contain direct evidence for event deposition by high-energy floods, including: (1) widespread upper- and transitional-upper flow regime elements; (2) frequent stacking of successively-lower flow-regime elements; (3) common subcritical subaqueous dune fields with superimposed ripple marks; (4) occasional thin, desiccated mudstones; and (5) evidence that microbial mats colonized substrates during intervals of sedimentary stasis. Together these strands of primary sedimentary geological evidence indicate that the alluvial deposition of the Meall Dearg Formation was typified by supercritical flows during high-energy floods, punctuated by prolonged intervals of sedimentary stasis. The preservation potential of all of the features was boosted by highly aggradational sedimentary conditions. These primary observations have implications for the 'norm' in pre-vegetation alluvium and confirm that, despite increasing recognition of diversity within Precambrian fluvial systems, classical pre-vegetation motifs of high-energy alluvial flood deposits preserved as "sheet-braided" alluvium are still an archetypal

sedimentary signature in some instances. Using supportive evidence from the Meall Dearg Formation, we recommend that the term "sheet-braided" be used in inverted commas in future studies; this emphasises the polygenetic depositional nature of the 20:1 width:thickness fluvial style, while maintaining the value of the term in the isolation of a key characteristic of pre-vegetation sedimentary architecture.

Keywords: Upper-flow regime; Supercritical; Chute and Pool; Antidune; Humpback cross-stratification; Stoer Group; MISS; "Sheet-braided"

1. THE TORRIDONIAN SANDSTONE AND PRE-VEGETATION ALLUVIUM

The 'Torridonian Sandstone' (or, simply 'the Torridonian') is the informal stratigraphic name for a >10 km thick succession of Proterozoic siliciclastic strata, overlying the Archean Lewisian gneiss complex, in the Highland region of northwest Scotland (Fig. 1). The Torridonian has been a well-studied unit of British regional stratigraphy for almost 200 years (e.g., MacCulloch, 1819; Sedgwick and Murchison, 1828; Peach et al., 1907). Its historical renown arises from both its wide geographic outcrop extent (200 km north to south; even greater at subcrop ((Blundell et al., 1985; Stein, 1988, 1992; Williams and Foden, 2011)) and status as the oldest unmetamorphosed sedimentary rock in the British Isles. During the last fifty years, numerous studies have concerned themselves with the sedimentary history of the succession (e.g., Selley, 1965; Williams, 1966, 2001; Gracie and Stewart, 1967; Stewart, 1969, 1982; Nicholson, 1993; McManus and Bajabaa, 1998; Owen and Santos, 2014; Ielpi and Ghinassi, 2015; Ielpi et al., 2016; Santos and Owen, 2016), its provenance and geochemistry (e.g., Stewart, 1991; Stewart and Donnellan, 1992; Van de Kamp and Leake, 1997; Young, 1999; Williams and Foden, 2011), and its palaeomagnetic (e.g., Stewart and Irving, 1974; Smith et al., 1983; Williams and Schmidt, 1997) and tectonostratigraphic (Kinnaird et al., 2007) characteristics. More recently, the succession has seen a revival of palaeobiological interest: microfossils extracted from Torridonian mudstones, first described by Teall (1907), have been deemed to the Earth's oldest

non-marine eukaryotes (Strother et al., 2011; Battison and Brasier, 2012; Brasier et al., 2016) and indirect evidence for early microbial life on land has been described (Prave, 2002; Callow et al., 2011; Strother and Wellman, 2016).

The Torridonian is also of global significance within a sedimentological context; containing some of the most extensive and easily-accessible successions of pre-vegetation alluvial strata worldwide. It is widely appreciated that river processes would have been markedly different before land plant evolution, supported by observations in poorly-vegetated modern catchments (e.g., Schumm, 1968; Fuller, 1985; Corenblit et al., 2015 ; Horton et al., 2017) and in the deep time alluvial stratigraphic record (Cotter, 1978; Davies and Gibling, 2010; Gibling et al., 2014; Davies et al., 2017a). A recent burst of geological investigations into pre-vegetation alluvium has been driven by a demand for a better understanding of economically-significant Precambrian and lower Palaeozoic hydrocarbon reservoirs and placer deposits, a search for terrestrial analogues for extraterrestrial alluvium on planets such as Mars, and context for the fossil record of the earliest life on Earth. A number of these studies have demonstrated the existence of a much greater variability of pre-vegetation fluvial styles than has traditionally been appreciated (e.g., Santos et al., 2014; Marconato et al., 2014; Ielpi and Rainbird, 2016a, 2016b; Santos and Owen, 2016) emphasising that further investigation of these anactualistic sedimentary systems is needed to fully appreciate the diversity of Precambrian alluvium.

This paper contributes new data to the global pool of pre-vegetation studies, through an original sedimentological analysis of the least-studied constituent unit of the Torridonian Sandstone: the Mesoproterozoic Meall Dearg Formation (MDF). Considering the long history of geological investigation into the region, and the number of studies that have focused on the more well-known alluvial formations of the Torridonian (e.g., the Applecross [Selley, 1965; Nicholson, 1993; Owen, 1995; Stewart, 2002; Owen and Santos, 2014; Ielpi and Ghinassi, 2015; Santos and Owen, 2016] and Bay of Stoer [Stewart, 1990; Stewart, 2002; Ielpi et al., 2016] formations), the MDF has remained largely overlooked. This is the first paper to explicitly address the sedimentary characteristics of the MDF, as only three studies have previously considered the

formation: Gracie and Stewart (1967) discussed sedimentary deposits at Enard Bay, Prave (2002) discussed putative microbially-induced sedimentary structures, and Stewart (2002) provided an overview of the MDF as part of a survey of the entire Torridonian. Other studies have overlooked the MDF, potentially because of its limited exposure (cropping out at only four locations; Rubha Réidh, Stoer, Balchladich Bay and Enard Bay) and dissection by the regionally-significant Coigach Fault (Fig. 1). Existing interpretations of the MDF have suggested that it was deposited by a sandy bedload-dominated fluvial system (Gracie and Stewart, 1967; Stewart, 2002). This paper revisits the formation in light of recent sedimentological advances, and discusses: (1) the architectural characteristics of the constituent sand-bodies of the MDF; (2) the spatial distribution of stratification types in accordance to established flow regime models; (3) the variety of preserved bedding plane features within the MDF; and (4) recurring facies that record prevailing sedimentary processes. These novel observations permit the interpretation of the MDF as recording distinct signatures of dominant high-energy alluvial event (and subordinate aeolian) sedimentation, preserved due to exceptional aggradational conditions.

2. STRATIGRAPHIC AND GEOLOGICAL CONTEXT

A detailed stratigraphy for the whole Torridonian is presented in Stewart (2002), and only a brief overview of the stratigraphic context of the MDF is discussed here. The Torridonian Sandstones comprise, from oldest to youngest, the Stoer, Sleat and Torridon groups (Fig. 1C); of which the MDF is the youngest constituent formation of the >2000 m-thick Stoer Group. The MDF succeeds the Bay of Stoer Formation and is unconformably overlain by the lacustrine Diabaig Formation of the Torridon Group. The Bay of Stoer Formation consists of dominantly fluvial, and subordinate interpreted aeolian (Park et al., 2002; Ielpi et al., 2016) sandstones. Specifically, the MDF succeeds the shallow lacustrine Poll a'Mhuilt Member of the Bay of Stoer Formation, apparently conformably. Lithostratigraphic correlation between the scattered outcrops of the MDF is permitted by their common stratigraphic position above the Stac Fada

Member of the upper Bay of Stoer Formation, which comprises a regionally-extensive event bed of meteorite-impact ejecta origin (Amor et al., 2008; Simms, 2015). However, the possibility remains that the units at each locality are not necessarily time equivalents. The MDF has not been directly dated, but its age is stratigraphically bracketed between 1177±5 Ma (Stenian Period of the Mesoproterozoic) and 977±39 Ma (Tonian Period of the Neoproterozoic), based on $^{40}Ar/^{39}Ar$ dating of the underlying Stac Fada Member and Rb-Sr whole-rock regressions of the overlying Diabaig Formation (Turnbull et al., 1996; Parnell et al., 2011). This age indicates that the MDF was deposited during the Grenvillian Orogeny, along the margins of the supercontinent Rodinia (Rainbird et al., 2012). This deposition on the edge of the Laurentian Shield meant that it largely avoided later Caledonian deformation (Williams and Foden, 2011).

The MDF is interpreted to have been deposited in a narrow rift basin with detritus sourced from local fault scarps (Stewart, 1982, 1990; Rainbird et al., 2001). Palaeomagnetic (Torsyik and Sturt, 1987) and geochemical (Stewart, 1990) data suggest deposition occurred in a semi-arid climate at a palaeolatitude of 10-20°N. A glacial setting was proposed for the lowermost Clachtoll Formation by Davison and Hambrey (1996), but evidence for this was disputed by Stewart (1997) and Young (1999).

3. SEDIMENTOLOGY OF THE MEALL DEARG FORMATION

Facies Associations

Two facies associations (FA) are recognised in strata of the MDF (Fig. 2). The facies associations are mutually exclusive, with FA1 cropping out at Rubha Réidh, Balchladich Bay and Stoer and FA2 at Enard Bay.

3.1. Facies Association 1 (Rubha Réidh, Balchladich Bay and Stoer)

Strata of FA1 form the majority of the exposed MDF, and all of the facies at Rubha Réidh, Balchladich Bay and Stoer. The contiguous Stoer-Balchladich Bay section is 200-300 m thick,

156 underlain by the Bay of Stoer Formation and unconformably overlain by the Applecross
157 Formation. At Rubha Réidh, the succession is truncated to 100 m thickness, with a faulted lower
158 contact and the Diabaig Formation unconformably overlain above (Stewart, 2002). FA1 consists
159 nearly entirely of sandstone (>99% of total strata). Mudstones (<1%) are restricted to mm-
160 thick, often desiccated, laterally discontinuous layers or intraformational mud clasts.
161 Sandstones are medium-grained, with the exception of the lowest 7 m of stratigraphy at Stoer,
162 where pebbly sandstones occur. Lower bounding surfaces are either flat (Fig. 3B), or drape and
163 preserve an underlying dune topography (Fig. 3C). Erosion between sand-bodies is restricted to
164 localized scours, no more than 50 cm deep. Various stratification types and bedding plane
165 features are present (Table 1). Three-dimensional outcrops permit the identification of both
166 foreset and backset (cross-stratification dipping up local palaeoflow) stratification and foreset
167 dips indicate that palaeoflow was towards 279° (n = 41). The description and interpretation of
168 each stratification type and bedding plane feature are as follows.

169 **3.1.1. Sandstone stratification types**

170 Stratification types in this section are documented in order of progressively decreasing
171 associated flow strength: their relative frequency of occurrence is shown in Figure 2.

172 **3.1.1a. Backset laminae associated with an upstream-dipping scour surface** *(Chute and*
173 *Pool structures)*

174 *Description* – Asymmetric scoured surfaces, filled by upstream-inclined cross laminae are
175 present at Rubha Réidh and Stoer (Fig. 4). Backsets truncate against steep, downstream-dipping
176 scoured margins, and are succeeded vertically by horizontal laminations and convex-up
177 bedding. At Stoer, convex-up bedding passes down-flow into horizontal laminations with soft-
178 sediment deformation structures (Fig. 4B).

179 *Interpretation* – Comparable features are rarely reported from the rock record (Fralick, 1999;
180 Fielding, 2006; Lowe and Arnott, 2016; Winston, 2016), but are analogous to chute and pool
181 structures formed in laboratory experiments (Alexander et al., 2001; Cartigny et al., 2014).

Chute and pool structures form due to a temporary hydraulic jump within a localized scour when shallow, faster flowing waters (the chute) pass immediately into deeper, slower flowing waters (the pool) (Fielding, 2006). Their relationship with juxtaposed bedforms in the MDF indicate that the pools were filled prior to flow waning to regimes associated with the deposition of antidune stratification and horizontal laminations. High-velocity and turbulent flow conditions account for the association of chute and pool structures with soft-sediment deformation.

3.1.1b. Convex-up bedding containing backset cross-laminae *(Antidunes)*

Description – Convex-up bedding is occasionally associated with otherwise horizontal beds (Fig. 5). Convex-up beds are low-relief (20 – 25 cm), symmetrical and internally characterized by cross-laminae that dip upstream (compared to palaeocurrents from nearby dune cross-stratification). They are solitary and do not form larger concavo-convex sets. Widths of convex-up portions range from 200 – 225 cm.

Interpretation – Symmetrical, convex-up beds with internal upflow-dipping cross-laminae suggest that they formed in the antidune stability field (e.g., Fielding, 2006; Cartigny et al., 2014). Antidune stratification has been produced in experimental flows underneath transient standing waves (e.g., Kennedy, 1963; Alexander et al., 2001), suggesting that standing waves developed in supercritical flow conditions during the deposition of the MDF. Their comparative scarcity compared with horizontal laminations (section 3.1.1c) reflects the transient nature of such flow conditions and the relatively low preservation potential of antidune stratification. Additionally, confident diagnosis of antidune stratification requires full preservation of the bedform under aggrading sedimentation (Cartigny et al., 2014), meaning that the number of identifiable antidune deposits in the MDF is likely an under-representation of their true abundance.

3.1.1c. Horizontal laminations *(Upper plane bed)*

Description – Horizontal laminations constitute the basal parts of the majority of FA1 sand-bodies (>95%) (Fig. 6; Fig. 8). Thin (< 4 mm), ungraded laminae occur in sets 5 – 110 cm thick. Sets are tabular in depositional-dip and strike sections. Underlying bounding surfaces are flat and exhibit no evidence of incision into the underlying bed (at outcrop scale). In large depositional-dip outcrops, planar laminations occasionally transition laterally to low-angle, down-flow dipping cross-stratification (section 3.1.1e).

Interpretation – Horizontal laminations record upper-flow regime plane bedding (Paola et al., 1989). Upward transitions from upper- to transitional upper-flow regime sedimentary structures are interpreted as the product of waning floods. Similarly, down depositional-dip transitions from horizontal laminations to low-angle cross stratification represent lateral decreases in flow strength (upper- to transitional upper-flow) (Fielding, 2006).

3.1.1d. Asymmetrical sigmoidal sets of cross-stratification *(Humpback dunes)*

Description – Cross stratification exhibiting a downflow-divergent sigmoidal geometry is present in multiple sand-bodies at Rubha Réidh (Fig. 6; Fig. 7A). The sigmoidal geometry permits the differentiation of discrete topset, foreset and bottomset elements. Convex-up bed topography is apparent at the top of each set (Fig. 7A); a stratification type referred to as humpback cross-stratification (Saunderson and Lockett, 1983; Fielding, 2006). Sets are up to 2.2 m high and can be traced down depositional-dip for > 65 m (Fig. 6). Ripple marks are frequently preserved in topographic lows associated with preserved convex-up topography (Fig. 6). In three-dimensional sections, it is clear that humpback sets comprise wedge-shaped packages that built out in a westwards direction (Fig. 7B).

Interpretation – Humpback 'form-sets' develop when deposition dominates over erosion at flow conditions transitional between the dune stability field and the upper plane bed field (Saunderson and Lockett, 1983). Convex-up bed topography at the top of each set implies that the bedforms are fully preserved ('form-sets') (Reesink et al., 2015).

3.1.1e. Low-angle (<20°) cross-stratification *(Transitional upper-flow regime dunes)*

Description – Low angle cross-stratification occurs throughout the MDF (Fig. 8A). Foreset dip angles range from 5° - 15°. In depositional-dip sections, low-angle foresets occasionally merge into horizontal laminations up-flow.

Interpretation – Low-angle cross-stratification develop at flow conditions transitional between dune stability field and upper plane bed stability (Fielding, 2006). Lateral transitions between horizontal laminations and low-angle cross stratification reflect localized variations in flow energy.

3.1.1f. High-angle (>20°) cross-stratification *(Lower flow-regime dunes)*

Description – Planar cross-stratification occurs in solitary sets of 10 - 30 cm thickness. Co-sets of planar cross-stratification do not occur; instead, sets are intercalated with sedimentary structures associated with upper-flow regime flows (most abundantly horizontal laminations) (Fig. 8B). Sets are highly tabular and show minimal lateral thickness changes in both depositional-dip and depositional-strike sections. Trough cross-stratification was only observed at the base of the formation at Stoer (coincident with the only pebbly interval observed in the MDF).

At Rubha Réidh, in instances where cross-bedded units occur at the top of a major sand-body, dune topography is preserved (Fig. 2; Fig. 3A; Fig. 9A). Dunes are spaced 0.5 - 1 .5 m apart and have heights of 10 - 30 cm. Abundant ripple marks are superimposed onto the dune microtopography (section 3.1.2a).

Interpretation – The migration of lower-flow regime two- and three-dimensional subaqueous dunes produce planar and trough cross beds respectively. The existence of tabular sets with minimal lateral variation in relief implies that flow depths were consistent across large areas. Co-sets of high-angle cross-stratification are entirely absent, with cross-stratification most

commonly occurring between upper-flow regime sedimentary structures suggesting their deposition relates to waning high-energy floods.

3.1.2. Bedding plane features

In the MDF, ripple marks and other sedimentary surface textures are common on some bedding surfaces, which record the preservation of primary substrates. Sedimentary surface textures exhibit a wide variety of morphologies, due to their formation on substrates that persisted for variable intervals of sedimentary stasis (Davies et al., 2017b). This morphological variability may hamper the determination of whether the textures had a microbial or abiotic origin, so in this section they are classified following the technique described in Davies et al., (2016): Category A structures are demonstrably abiotic in origin; Category Ba is used where circumstantial evidence suggests structures may be biotic, but an abiotic origin cannot be ruled out; Category Ab is used for the opposite situation to this; Category ab is used where there is no clear evidence to support abiotic or biotic origin.

3.1.2a Ripple-Marks

Description – Symmetrical ripple-marks are nearly ubiquitous on each studied planform surface (n = 12) at Rubha Réidh, Balchladich Bay and Stoer (Fig. 9). The largest of these exposed surfaces has an area of >1000 m^2. Ripple-marks are frequently seen superimposed on top of dune topography, where they have weakly anastomosing sinuous crests which rarely extend > 2 m (Fig. 9A). On flat surfaces which lack dune microtopography, crests are subparallel and extend for > 10 m (Fig. 9B). Ripple-marks record unidirectional flow on individual bedding planes, but a near 360° dispersal is apparent when all rippled surfaces are considered (Fig. 9B). The modal E-W strike-line is perpendicular to the prevailing westward flow (θ = 279°; n = 41). Many ripple marks have clear drainage lines etched into their flanks, indicating emergence and drainage subsequent to their formation (Fig. 10A, 10B). Crests are mostly well-rounded or flat-topped. Sharp crested ripple marks are rare (Fig. 10C), and contain synaeresis cracks within

their troughs (Fig. 10D). Infrequent interference ripple-marks occur (Fig. 10E). Ripple-marks located within dune troughs are often draped by mud (Fig. 10F).

In addition to planform exposures of ripple-marks, trains of ripple crests can be observed within vertical sections (Fig. 6; Fig. 10G). Above humpback dunes, sharp crested ripple-marks are present in dune troughs and form ripple trains which extend laterally for up to 4 m (Fig. 6). In rare instances ripple crests display uneven oversteepening (Fig. 10H).

Interpretation – Symmetrical ripple-marks record bedform stability under low flow regime: representing falling flood stage. Their near-ubiquitous positioning above sand-bodies that contain upper- and transitional-upper flow regime sedimentary structures suggests that flood waters receded to leave pools of standing water across the depositional plain. Their comparatively greater abundance within humpback dune troughs (compared with crests) lends further credence to this notion, suggesting more pervasive pooling of water within pre-existing topographic lows. Variations in ripple-crest strike-line suggest that this ponded water drained and moved in different directions, depending on localized slope and wind conditions. Soft sediment deformation of some ripple crests may have been caused by current drag over the rippled surface during subsequent flooding events. Alternatively the oversteepening may be seismically induced.

3.1.2b Adhesion Marks (A)

Description – Adhesion marks are frequently seen to be superimposed upon ripple-marked surfaces (Fig. 11). They present as 2 – 5 mm wide, 1 – 3 mm high positive epirelief mounds that are irregular in form (i.e., adhesion marks and not adhesion ripples; Kocurek and Fielder, 1982). Their spatial distribution across any given bedding surface is strongly dependent on the associated dune and ripple microtopography (Fig. 11). On dune crests (topographic highs), ripple-marks are densely blanketed by adhesion marks across their crests and troughs (Fig. 11A). Within dune troughs (topographic lows), adhesion marks are only ever restricted to ripple crests, or are absent entirely (Fig. 11B). On flat beds lacking dune microtopography,

adhesion marks occur on both ripple crests and troughs, but are more common on the former (Fig. 11C).

Interpretation – Adhesion marks indicate that water-lain sands were intermittently subaerially-exposed, permitting the accretion of wind-blown sand grains onto moist substrates (Kocurek and Fielder, 1982). Adhesion marks are progressively more common with height above the surface (i.e., most common on ripple crests on dune crests; least common in ripple troughs in dune troughs), indicating that they can be used to locally determine how extensive the recession of pooled water was between flood events. The total absence of adhesion marks in some dune troughs suggests that, in some instances, no subaerial exposure occurred and that pooled water persisted until the subsequent flood event (Fig. 11A-C).

3.1.2c Sinuous shrinkage cracks (*Manchuriophycus*) (Ba)

Description – Sinuous shrinkage cracks were observed at one ripple-marked surface at Rubha Réidh. Cracks are up to 1 cm wide and 25 cm long. They most commonly occur within, and parallel to, ripple troughs, but individual cracks may also cross ripple crests (Fig. 12). They are preserved in positive epirelief, although post-depositional erosion often results in accompanying negative epirelief impressions.

Interpretation – The sinuous shrinkage cracks fit the type description of the "pseudofossil" *Manchuriophycus* (Endo, 1933). *Manchuriophycus* has variously been interpreted as fossilized algae, a burrow structure, or inorganic desiccation crack (see Hantzschel, 1962); though is now more commonly thought a type of microbially-induced sedimentary structure (*sensu* Noffke et al., 2001) arising due to the shrinkage of microbial mats with very high strengths and elasticity (Koehn et al., 2014). In the absence of a mat, grains would more likely have accommodated stress by moving past one another rather than opening cracks (McMahon et al., 2016). If the MDF examples have a microbial origin, their preferential development in ripple troughs would imply that matgrounds were thicker within topographic lows (Schieber, 2007).

Prave (2002) reported similar features ('irregular- to rod-shaped fragments of variable length and curvature concentrated within ripple troughs', p. 813) and interpreted these as fragments of microbially bound sand layers that had been entrained and rolled during ephemeral flows (his Fig. 4A). Surfaces with well-formed *Manchuriophycus* identified during this study also host positive epirelief fragments similar in morphology to the fragments described by Prave (2002) (Fig. 12).

3.1.2d Reticulate Markings (Ba)

Description – Reticulate ridges occur on multiple planform surfaces (Fig. 13A; Fig. 13B). Individual nets are 2 – 6 mm wide and 1 – 2 mm high.

Interpretation – Reticulate markings have modern analogues in cyanobacteria and eukaryotic algae, where they arise from filament tangling (Shepard and Sumner, 2010; Davies et al., 2016).

3.1.2e Serrated margins (ab)

Description – In rare instances, clear serrated margins several millimeters thick separate bedding plane surfaces with and without adhesion marks (Fig. 13C).

Interpretation – Prave (2002) interpreted the serrated margins as remnants of microbially bound layers, where sand grains had adhered to a microbial crust (due to the presence of sticky extracellular polymeric substances and cyanobacterial filaments). Possible alternative abiotic explanations for the margins could include: (1) post-depositional partial erosion of overlying sediment layers; or (2) original patchy distribution of moist sands resulting in localized adhesion.

3.1.2f Desiccated Sandstone (ab)

Description – In rare instances, desiccated polygons overprint ripple marks without a muddy matrix (Fig. 14A). Polygons are 15 - 25 cm wide and a few centimeters deep.

355 *Interpretation* – Desiccation cracks only develop in materials with sufficient cohesive strength
356 (e.g., van Mechelen, 2004). Within moist (abiotic) sands, such cohesion can only be attained if
357 grains have high textural maturity (Chavdarian and Sumner, 2011; Glumac et al., 2011). To date,
358 desiccation experiments on clay-poor sand substrates with angular grains have been
359 unsuccessful (Kovalchuk et al., 2016). However, microbiota can increase sand cohesion by
360 stabilizing grains with cyanobacterial filaments and extracellular polymeric substances (e.g., De
361 Bore, 1981) and, in doing so, enable polygon formation (Prave, 2002; Eriksson et al., 2007;
362 Kovalchuk et al., 2016; McMahon et al., 2016). Whilst this is a viable formation mechanism, the
363 absence of proximal microbial fabrics on the desiccated sandstone bed at Rubha Réidh means
364 that no direct evidence for a microbial origin has been conclusively ascertained in this study.

365 **3.1.3 Desiccated Mudstone**

366 *Description* – The mudstones that account for <1% of FA1 are ubiquitously desiccated, with
367 individual polygons up to 1 m in diameter (Fig. 14B).

368 *Interpretation* – Desiccated mudstones result from a reduction in volume as muds dry out when
369 emerged (Bradley, 1933), indicating that all the preserved Meall Dearg mudstones were
370 deposited immediately prior to subaerial exposure.

371 **3.1.4 Interpretation of Facies Association 1** *(High energy alluvial events)*

372 Sand-bodies at Stoer, Rubha Réidh and Balchladich Bay are interpreted as the deposits of
373 multiple high-energy alluvial flood events. During peak flow, upper-flow regime conditions
374 prevailed (Fielding, 2006), occasionally entering the chute and pool or antidune stability
375 regimes (Alexander et al., 2001; Cartigny et al., 2014). As floods waned, flows progressively
376 operated under transitional upper- and subcritical flow-conditions, resulting in the vertical
377 stacking of sedimentary structures in accordance to decreasing flow velocity (Fig. 2). At Stoer,
378 stratification types are typically limited to intercalated horizontal laminations and planar cross-
379 stratification, with each package the result of an individual flood. Packages at Stoer are rarely

greater than 20 cm thick, implying either shallow flow depths or partial erosion by successive flood events. This is in contrast to the variety of preserved stratification at Rubha Réidh, where humpback form-sets are up to 2.2 m thick and must have been submerged in deeper water during deposition. During high flood stages, it is implicit that the critical flow velocity for coarse-sediment transport was exceeded, so the absence of such sediment grades indicates either: (1) only medium-grained sediment in the primary sediment supply (e.g., due to a significant distance from the sediment source); or (2) bypass of coarser sediment fractions. Variably-striking ripple crestlines are superimposed on nearly all studied sand-bodies reflecting unconfined post-flood pooling of quiescent waters.

Abundant adhesion marks and desiccation cracks indicate intermittent subaerial exposure. The diversity of reticulate markings, *Manchuriophycus*, and other surface textures with ambiguous origin, offer strong circumstantial evidence for microbial colonization of substrates during sedimentary stasis (Schieber, 1999; Prave, 2002; Davies et al., 2016).

No apparent unconformity exists between the MDF and the underlying Bay of Stoer Formation, but the boundary marks a major change in sedimentary lithofacies. Bay of Stoer Formation fluvial facies consist of stacked, lower flow-regime, three-dimensional sedimentary structures (Stewart, 2002; Ielpi et al., 2016), typical of perennial fluvial flow (Bristow, 1987; Best et al., 2003), and are overlain by the shallow lacustrine Poll a'Mhuilt Member (Stewart, 2002). In contrast, MDF deposition occurred as high energy events; a lithofacies shift that probably reflects changes in the regional temperature and seasonality of precipitation (e.g., Fielding, 2006; Lowe and Arnott, 2016), within the low-latitude, semi-arid climate belt where the formation was deposited (Torsvik and Sturt, 1987; Stewart, 1990). Alternatively, the stratigraphic appearance of these features may be a preservational artefact related to changes in basin accommodation, but, as the duration of hiatus at the Poll a' Mhuilt-Meall Dearg boundary is not understood, such a control cannot be confidently assessed.

406 **3.2. Facies Association 2** *(Enard Bay)*

407 The 150-250 m thick MDF succession at Enard Bay overlies the Poll a' Mhuilt Member (not
408 exposed in continuous coastal section) and is unconformably overlain by the Diabaig Formation
409 (Stewart, 2002). Due to lithofacies dissimilarity, Gracie and Stewart (1967) and Stewart (2002)
410 did not correlate these strata with those described in Section 3.1., but the locality is now the
411 British Geological Survey reference section for the MDF (BGS Lexicon of Named Rock Units
412 [online] accessed 2017). Here, the Enard Bay strata are recorded as Facies Association 2. FA2
413 deposits are near-ubiquitously composed of fine- or medium-grained sandstones (Fig. 2; Fig.
414 15A; Fig. 17B). No mudstones were observed in this study. Planar cross-beds occur in sets 1 – 5
415 m thick, intercalated with laterally extensive planar beds up to 2.8 m thick (Fig. 15A; Fig. 15B).
416 These sedimentary characteristics indicate an aeolian origin for FA2, which was likely deposited
417 coevally to the FA1 alluvial deposits. Although an aeolian interpretation was previously
418 discarded by Stewart (2002) on the basis that 'convex upward aeolian reactivation surfaces
419 comparable in size with those figured by McKee (1967) were not observed' (p. 72), an absence
420 of such features is not diagnostic proof against aeolian deposition. Two sedimentary facies are
421 described, in support of an aeolian origin: [1] Large-scale planar cross-bedded; and [2] Planar-
422 bedded. These facies are exclusive of the southernmost outcrop currently mapped as MDF; a
423 singular exposure of occasionally pebbly, coarse-grained, cross-bedded sandstone separated
424 from the described succession by 250 m (Krabbendam, 2012). This c. 5 metre-high and c. 30
425 metre-wide partially exposed outcrop forms a prominent small knoll, apparently faulted into
426 contact with the rest of the MDF at Enard Bay (Fig. 16). Given the dissimilarity of its facies to
427 the remainder of the succession, the inability to confirm a genetic relationship with the rest of
428 the MDF strata at Enard Bay, and the local presence of faulted slivers of pebbly sandstones of
429 the Applecross Formation, the exposure is here considered most likely to be a previously
430 unrecognized outcrop of the latter formation. However, even if the outcrop records a basal
431 pebbly fluvial facies with the remainder of the local MDF, this lithology is never seen to be
432 interbedded with the overlying aeolian facies.

3.2.1 Large-scale planar cross-bedded sandstones *(Aeolian dunes)*

Description – Large-scale planar cross-bedding occurs within fine- to medium-grained well-rounded arkosic arenites. Cross-beds occur in sets of 1.2 – 5 m thickness (Fig. 15A), which are planar in depositional-dip sections (Fig. 15B) and curved in depositional-strike sections (Fig. 15C). Curved foresets demonstrate palaeoflow spreads of up to 40° across individual sets (Fig. 15D, Fig. 15E), although the dispersal does not detract from the highly-unimodal WSW-directed stacking of dune foresets (θ = 248°, n = 201). Individual sets are up to 40 m wide, with typical angles of climb between 15 – 25° (maximum 34°). Individual foresets are characterized by 1 – 4 mm thick, steeply dipping cross laminae with subtle inverse grading (Fig. 17A) or planar laminae with no discernible grain-size trends (Fig. 17B). Cross-bedded sets are typically bound by planar bedded sandstones (see Section 3.2.2; Fig. 15A; Fig. 15B). When planar-beds are absent, dune sets are separated by low-angle, erosional reactivation surfaces (Fig. 18A).

Interpretation – The presence of fine- to medium-grained sandstones with well-rounded grains, arranged in cross-strata sets that are composed of cross-laminae (grainflow) and planar laminae (grainfall) suggests that the planar cross-bedded facies represent aeolian dune deposits (e.g., Hunter, 1977; Kocurek, 1981, 1996). High dispersal of palaeoflow measurements across individual dune sets, and curved crest lines (Fig. 15C) suggest that the dunes were arcuate.

3.2.2 Planar-bedded sandstones *(Aeolian interdunes)*

Description – Planar-bedding occurs in packages of fine- and subordinate medium-grained arkosic arenites, 0.1 – 2.4 m thick, and display near ubiquitous pin-stripe lamination (Fig. 17D). Adhesion lamination is uncommon (Fig. 17E). Planform surfaces are largely featureless, but sometimes contain adhesion marks (Fig. 17F) or, rarely, poorly developed ripple marks (n = 4) exhibiting a near 90° spread of strike lines.

Within the planar-bedded facies, one known example of a coarse-grained, apparently massive channelized sand-body incises into a 2.4 m thick planar-bedded package (Fig. 18B). Exposure

458 constraints restrict full dimensions from being determined, but the preserved sand-body is at
459 least 9 m wide and has a relief of 1.5 m.

460 *Interpretation* – Planar-bedded facies are interpreted as aeolian interdunes. Pin-stripe
461 lamination and climbing ripple stratification can form by aeolian ripple migration under
462 aggrading conditions (Fryberger et al., 1988; Hunter, 1977). Adhesion marks record moist
463 interdune surfaces. The interpreted interdune packages are comparatively thinner
464 (predominantly <1 m, maximum 2.4 m) and less laterally extensive than dune surfaces. The
465 channelized sand-body may be (the only) evidence for fluvial deposition in FA2, but the absence
466 of internal structure forbids further interpretation. If fluvial in origin, it differs from the FA1
467 alluvium at Rubha Réidh, Balchladich Bay and Stoer through its coarser grain size and presence
468 of channel margins.

469 **3.3. Mutual exclusion of aeolian and fluvial deposits**

470 The mutual geographic exclusion of the aeolian facies association at Enard Bay (FA2) and fluvial
471 facies association at Rubha Réidh, Balchladich Bay and Stoer (FA1) is not unexpected. In many
472 modern mixed fluvial-aeolian systems, there is a high propensity for fluvial flood-reworking of
473 neighbouring aeolian dune deposits (e.g., Kocurek and Nielsen, 1986; Langford, 1989), biasing
474 the resultant sedimentary record towards alluvial dominance. This preservation bias may have
475 been particularly acute in pre-vegetation systems, when plant-related factors that can buffer
476 against reworking (such as sediment binding and baffling by roots, and the reduction of near-
477 surface flow velocities by above-ground structures) were absent (Tirsgaard and Øxnevad, 1998;
478 Rodriquez et al., 2014). Furthermore, wind-blown sands may have been more readily deflated
479 from the alluvial realm in the absence of vegetation (Dalrymple et al., 1985; Lancaster and Baas,
480 1998; Mountney, 2004). Deflation may also have been locally promoted by a low groundwater
481 table (as suggested by the absence of wet interdune facies in the MDF) (Fryberger et al., 1988;
482 Kocurek and Havhom, 1993; Tirsgaard and Øxnevad, 1998). In such a scenario, the aeolian
483 strata at Enard Bay would represent exceptional preservation of deposits that were originally

484 more common when the MDF depositional environments were active; their absence at Rubha
485 Réidh, Balchladich Bay and Stoer reflecting the biasing effects of high-energy flood events. The
486 limited outcrop of the MDF at Enard Bay does not permit a robust explanation for their
487 exceptional preservation to be determined, but any one of a number of potential preservation
488 mechanisms may have been responsible (e.g., relating to climate, sediment supply, rate of dune
489 migration or accommodation space generation; Mountney, 2012).

490 **4. DISCUSSION**

491 **4.1. Architectural analysis in outcrop of limited exposure**

492 Where extensive along-strike and down-dip exposure of alluvial strata exists, architectural-
493 element analysis (e.g., Miall, 1985; Long, 2011) can be a powerful conceptual tool for elucidating
494 geomorphic and planform components of pre-vegetation river systems (e.g., Long, 2006; Ielpi
495 and Rainbird, 2015). However, such outcrop quality is not universal to all pre-vegetation
496 alluvial successions. The MDF provides a useful case-study in the importance of taking a
497 conservative approach by making interpretations of alluvial strata based only on observable
498 geological phenomena in the field. The formation contains sufficient primary sedimentary
499 geological signatures to conclusively affirm its deposition by high-energy floods, but its outcrop
500 quality and accessibility is unsuited for any robust interpretation of fluvial planform. In this
501 discussion, we emphasise (1) that the outcrop quality of the MDF is not unusual for strata of
502 Mesoproterozoic age and that the use of succession-scale architectural analysis on this unit, or
503 similarly-exposed units, is inappropriate; and (2) in instances such as this, the term "sheet-
504 braided" (used in inverted commas, and only when diagnostically-applicable) is useful
505 descriptive nomenclature, confirming the distinct nature of pre-vegetation alluvium.

506 **4.1.a. Limitations of determining alluvial architectural style in the Meall Dearg Formation**

507 The MDF is unsuited for succession-scale architectural analysis due to the nature of its outcrop.
508 Its maximum along-strike exposure is 50 metres at Enard Bay and 140 metres at Stoer. These
509 maximum exposures are dissected by multiple local faults and joints, rendering it rarely
510 possible to trace stratigraphic bounding surfaces along their original extent. Large-scale

depositional architectures are unsuited for interpretation from satellite imagery, as has been undertaken for older units of the Stoer Group (Ielpi et al., 2016), for three reasons: (1) The strata are tectonically inclined between 25-30° and have a NNE strike (Fig. 19A). Vertical observation of beds that crop out obliquely in plan-view greatly exaggerates true bed thickness and means that successive bounding surfaces are laterally offset; (2) Coastal exposure disappears underneath a variably deep cover of post-glacial till and peat bog within metres east of the coast (Fig. 19B). Topographic mapping cannot trace beds beneath this drift as its relief is not influenced by the depositional stratigraphic architecture of the underlying, lithologically homogenous formation; (3) Key stratigraphic contacts are variably obscured by local jointing, weathering, beach debris, vegetation, and intertidal algae. We deliberately refrain from making any inference of ancient fluvial planform for the MDF as any such 'interpretation' would be speculative and methodologically distinct from the robust interpretation of high-energy flood deposition, made from primary field observation.

4.1.b. "Sheet-braided" fluvial style: a polygenetic architectural signal of Precambrian alluvium

While the outcrop quality of the MDF prohibits a refined architectural assessment of the unit, the exposure is still of sufficient quality to recognize that its constituent alluvial sandbodies exhibit an almost uniform "sheet-braided" architecture (*sensu* Cotter, 1978). The term "sheet-braided" was introduced by Cotter (1978) for individual genetic units of sandstone with width:depth ratios greater than 20:1. His original definition explicitly stated that "sheet-braided" was a subdivisional classification of the 'fluvial style' of an alluvial sedimentary package (Cotter, 1978, p. 364), and that 'fluvial style' referred to the character of an alluvial *rock sequence* (Cotter, 1978, p. 362), independent of any conceptual models of fluvial planform for the depositional environment of a given unit. This strict definition of the term was maintained in the three decades after Cotter's (1978) work, and was reiterated by Davies & Gibling (2010) and Davies et al. (2011). Recently, however, the term has increasingly become conflated as having geomorphological significance for original fluvial planform, and a number of papers have

538 referred to ‘sheet-braided rivers’ (e.g., Ielpi and Ghinassi, 2015; Ielpi and Rainbird, 2016b; de
539 Almeida et al., 2016). The inclusion of the word ‘braided’ in Cotter’s (1978) term is thus
540 unfortunate, due to the confusion between geomorphology and sedimentology that has
541 subsequently arisen.
542 In response to this conflation of geomorphological form and sedimentary product, a number of
543 papers have argued against the predominance of “sheet-braided” Precambrian alluvium, on the
544 basis that special circumstances of outcrop and exposure may permit a more refined
545 interpretation of fluvial planform during deposition (e.g., Ielpi and Rainbird, 2015, 2016a,b;
546 Santos and Owen, 2016). However, even when such interpretations are possible, most
547 examples of Precambrian alluvium remain “sheet-braided” *sensu* Cotter (1978) (e.g., minimum
548 30:1 aspect ratio foreset bar sandbodies; Ielpi and Rainbird, 2016b; 20:1 to 80:1 channel
549 sandbodies; Ielpi and Ghinassi, 2015). Such “sheet-braided” fluvial style is clearly polygenetic:
550 applying the original definition, examples are known where the architecture has developed
551 deposited by highly mobile channels (e.g., Todd and Went, 1991; Rainbird, 1992; McMahon et
552 al., 2017), exceptionally wide channels (e.g., Fuller, 1985; Nicholson, 1993), deep channelled
553 drainage (Ielpi and Rainbird, 2016b; Ielpi et al., 2016), unconfined flow (e.g., Winston, 2016)
554 and high-energy flood events (Tirsgaard and Øxnevad, 1998; this study).
555 Despite these issues, we contend that the term still has value, providing that it is used as a
556 passive descriptor of architectural properties rather than carrying implications of
557 palaeoenvironmental setting. The first factor in support of the retention of the term is that in
558 many natural geological outcrops, such as those of the MDF, the low diagnostic bar for the
559 identification of “sheet-braided” architecture (>20:1 aspect ratio) means that this architectural
560 characteristic can still be identified or rejected, even when more refined architectural
561 interpretation is prohibited. The second factor in support of its retention is that the
562 characteristic retains importance as a key distinction between alluvium deposited before and
563 after the evolution of land plants: the ubiquity of “sheet-braided” alluvium in Precambrian
564 strata means that it may be mistakenly perceived as a bucket term, but its true merit lies in the

converse fact that there are no known examples of post-Silurian alluvial successions that are dominated by such architecture. Thus, in a holistic view of alluvium through time, the Precambrian dominance and Phanerozoic diminishment of "sheet-braided" alluvium attests to the significance of the evolution of a terrestrial flora in promoting a wider diversity of preserved alluvial phenomena.

In order to maintain these clear practical and conceptual uses, we propose that the term "sheet-braided" should continue to be applied in studies of ancient alluvium, but that it should be used in inverted commas in future studies, in recognition of the fact that the term is applicable to a variety of polygenetic alluvial strata and is not necessarily diagnostic of a braided fluvial planform at the time of deposition. Despite the potentially confusing inclusion of the word 'braided' in the term, its continued usage is preferential to the adoption of new terminology because: (1) the term "sheet-braided" is already entrenched in published literature; (2) any new terminology would require reference to the 'sheet' form of the strata, but sedimentological terminology invoking this term is already congested and requires careful application (North & Davison, 2012); and (3) the inherent fuzziness of the rock record, the vagaries of outcrop exposure and preservation, and the need for revision of concepts as new observations are made, mean that the science of sedimentary geology is necessarily pragmatic in its terminology: there is strong precedent for the retention of terms that no longer carry the implicit interpretation apparent in their wording (e.g., synaeresis cracks (McMahon et al., 2016), the sedimentary structure 'Kinneyia' (Davies et al., 2016), various ichnological and ichnofacies terms (Minter et al., 2016)). We emphasise that the term should always be used in conjunction with more detailed analysis when outcrop quality permits and that it is not exclusive of other, more refined classification schemes (e.g., Krynine, 1948; Friend et al., 1979, Friend, 1984; Gibling, 2006).

Improved adoption of the term "sheet-braided" in its original sense (Cotter, 1978) will promote the comparability of different studies, paving the way for a better understanding of the truly unique characteristics of pre-vegetation alluvium and the Palaeozoic transition away from "sheet-braided" ubiquity. A better understanding of the global and stratigraphic distribution of

592 "sheet-braided" alluvium will potentially shed light on the extrinsic factors that determined why
593 this *fluvial style* was apparently such a common geological signature of a variety of different pre-
594 vegetation *fluvial systems*.
595
596 **4.2. Aggradation and stasis during deposition permit the identification of high-energy**
597 **flood events**
598
599 Preserved Meall Dearg stratification types and sedimentary surface textures have enabled the
600 identification of high-energy flood events, but this interpretation was only permitted because
601 the strata contain direct evidence for: (1) upper-flow regime bedforms deposited by rapidly
602 decelerating flows under highly aggrading bed conditions; and (2) bedding plane records of
603 intervals of sedimentary stasis.

604 Upper-flow regime bedforms such as antidunes have traditionally been considered to be
605 transient sedimentary features, with limited long-term preservation potential (e.g., Reid &
606 Frostick, 1994). However, they can be preserved, unmodified, when the rate of deceleration
607 does not permit bedforms to equilibrate with flow regime (McKee et al., 1967; Alexander and
608 Fielding, 1997; Alexander et al., 2001); conditions that may have been more frequent during
609 Earth history than has traditionally been assumed (Fielding, 2006). The stacking of stratification
610 types recording progressively lower-flow regime conditions, as can be seen in the MDF, is
611 attributable to such conditions of rapid sediment fall-out during falling flood stages. The
612 preservation of these signatures, in addition to the full preservation of convex lamina sets
613 within antidunes, attests to high rates of bed aggradation during sedimentation (Alexander and
614 Fielding, 1997; Fielding, 2006; Cartigny et al., 2014).

615 The exceptional aggradational preservation of antidunes and related bedforms provides direct
616 evidence that supercritical flow conditions developed during alluvial deposition, but cannot
617 determine whether such conditions were perennial or whether they instead reflect discrete

high-energy flood events. The determination of event deposition requires separate evidence that the sedimentary system repeatedly reverted to background conditions of low flow regime or sedimentary stasis (neither deposition nor erosion; Tipper, 2015) subsequent to the development of supercritical flow. In the MDF, the packages of sediment revealing supercritical flow are sandwiched between strata that preserve bedding plane evidence for prolonged intervals of sedimentary stasis. Such features include sedimentary surface textures of both abiotic (adhesion marks and desiccation cracks) and likely microbial origin (e.g., reticulate marks, *Manchuriophycus*), analogous to modern features that develop during sedimentary stasis in ephemeral streams (Davies et al., 2017b). In order for such original substrate features to have become preserved in the sedimentary record, the succeeding flows must have lacked the capacity to erode the underlying substrate. In sparsely-vegetated modern and ancient ephemeral alluvial settings, rapidly aggraded sediment piles can change the locus of subsequent sedimentary events, thus escaping erosional truncation (Field, 2001; Cain and Mountney, 2009). In the MDF, evidence for such conditions can be seen in the way in which bounding surfaces are rarely erosional; succeeding packages of strata, most often floored with upper-flow regime elements, are deposited directly above preserved topography (Fig. 3). This indicates that, despite the surpassing of a critical threshold for the deposition of upper flow bedforms, the critical threshold for erosion of underlying strata was not exceeded. The only erosional contacts in the entire succession are restricted to laterally discontinuous <50 cm scour-cuts. These characteristics of the MDF suggest that highly aggrading bed conditions can enhance the preservation potential of strata recording sedimentary stasis, in addition to supercritical bedforms.

5. CONCLUSION

The spatial distribution of stratification types and bedding plane features across the Mesoproterozoic Meall Dearg Formation indicate deposition by high energy alluvial events and, subordinately, as aeolian dunes. The alluvial and aeolian sedimentary facies are mutually

644 exclusive: potentially suggesting aeolian sediments were only preserved in regions less prone to
645 reworking by alluvial activity. The "sheet-braided" alluvial sandstones contain a variety of
646 stratification types relating to upper-flow (chute and pool structures, antidune stratification,
647 horizontal laminations), transitional upper-flow (humpback cross-stratification, low-angle cross
648 stratification) and lower flow-regime conditions (planar cross-stratification, trough cross-
649 stratification, ripple marks). Bedding surfaces separating major sand-bodies include primary
650 substrates that host desiccation cracks, adhesion marks and putative microbial sedimentary
651 surface textures (e.g., *Manchuriophycus,* reticulate marks), which developed during prolonged
652 intervals of sedimentary stasis. The vertical stacking of sedimentary structures in accordance
653 with decreasing associated flow velocity, as well as evidence of periodic emergence and non-
654 deposition, suggests event sedimentation during episodic floods. This degree of interpretation
655 was only achievable due to specific sedimentary conditions at the time of deposition; namely
656 the combination of (1) rapidly decelerating flows acting under aggrading bed conditions; and
657 (2) intervals of non-deposition, during which primary sedimentary surface textures were
658 imparted onto the substrate. Confidence in the interpretation of these depositional processes
659 was attainable despite the fact that the outcrop quality of the Meall Dearg Formation renders it
660 unsuitable for detailed architectural analysis. In order to promote further robust
661 interpretations from pre-vegetation alluvium of limited outcrop extent, we suggest that the
662 term "sheet-braided" (in inverted commas) continues to be applied or rejected, in order to
663 ensure that the nature of pre-vegetation alluvium may be assessed from worldwide outcrops of
664 varying quality, without recourse to over-interpretation. The depositional characteristics of the
665 Meall Dearg Formation are in line with classical facies models for pre-vegetation alluvium, but
666 we emphasise that our observations do not reveal universal characteristics of Precambrian
667 rivers: they reflect one of a multitude of depositional conditions that could lead to the
668 deposition of "sheet-braided", pre-vegetation alluvium.

669

Acknowledgments and Funding

Supported by Shell International Exploration and Production B.V under Research Framework agreement PT38181. Two anonymous reviewers and editor Adrian Hartley are thanked for comments which improved the manuscript.

690 **References**

691 Alexander, J., Bridge, J. S., Cheel, R. J., & Leclair, S. F. (2001) Bedforms and associated
692 sedimentary structures formed under supercritical water flows over aggrading sand beds.
693 *Sedimentology*, 48, 133-152.

694 Alexander, J., & Fielding, C. (1997). Gravel antidunes in the tropical Burdekin River, Queensland,
695 Australia. *Sedimentology*, *44*(2), 327-337.

696 Amor, K., Hesselbo, S. P., Porcelli, D., Thackrey, S., & Parnell, J. (2008) A Precambrian proximal
697 ejecta blanket from Scotland. *Geology*, 36, 303-306.
698 Battison, L., & Brasier, M. D. (2012) Remarkably preserved prokaryote and eukaryote
699 microfossils within 1Ga-old lake phosphates of the Torridon Group, NW Scotland. *Precambrian*
700 *Research*, 196, 204-217.
701 Best, J.L., Ashworth, P.J., Bristow, C.S., Roden, J., 2003. Three-dimensional sedimentary
702 architecture of a large, mid-channel sand braid bar, Jamuna River, Bangladesh. Journal of
703 Sedimentary Research 73, 516-530.
704 Blundell, D. J., Hurich, C. A., & Smithson, S. B. (1985) A model for the MOIST seismic reflection
705 profile, N Scotland. *Journal of the Geological Society*, 142, 245-258.

706 Bradley, W. H. (1933). Factors that determine the curvature of mud-cracked layers. *American*
707 *Journal of Science*, (151), 55-71.

708 Brasier, A. T., Culwick, T., Battison, L., Callow, R. H. T., & Brasier, M. D. (2016) Evaluating
709 evidence from the Torridonian Supergroup (Scotland, UK) for eukaryotic life on land in the
710 Proterozoic. *Geological Society, London, Special Publications*, 448.

711 Bristow, C.S., 1987. Brahmaputra River: channel migration and deposition.
712 Callow, R. H., Battison, L., & Brasier, M. D. (2011) Diverse microbially induced sedimentary
713 structures from 1Ga lakes of the Diabaig Formation, Torridon Group, northwest Scotland.
714 *Sedimentary Geology*, 239, 117-128.

British Geological Survey Lexicon of Named Rock Units [online resource] http://www.bgs.ac.uk/lexicon/lexicon.cfm?pub=TAD. Accessed 5th May 2017.

Cartigny, M. J., Ventra, D., Postma, G., & Den Berg, J. H. (2014) Morphodynamics and sedimentary structures of bedforms under supercritical-flow conditions: New insights from flume experiments. *Sedimentology*, 61, 712-748.

Chavdarian, G. V., & Sumner, D. Y. (2011). Origin and evolution of polygonal cracks in hydrous sulphate sands, White Sands National Monument, New Mexico. *Sedimentology*, *58*(2), 407-423.

Corenblit, D., Davies, N. S., Steiger, J., Gibling, M. R., & Bornette, G. (2015). Considering river structure and stability in the light of evolution: feedbacks between riparian vegetation and hydrogeomorphology. *Earth Surface Processes and Landforms*, *40*(2), 189-207.

Cotter, E., 1978. The evolution of fluvial style, with special reference to the central Appalachian Paleozoic. In: Miall, A.D. (Ed.), Fluvial Sedimentology: Canadian Society of Petroleum Geologists Memoir, vol. 5, 361–383.

Dalrymple, R. W., Narbonne, G. M., & Smith, L. (1985). Eolian action and the distribution of Cambrian shales in North America. *Geology*, *13*(9), 607-610.

Davies, N. S., & Gibling, M. R. (2010) Cambrian to Devonian evolution of alluvial systems: the sedimentological impact of the earliest land plants. *Earth-Science Reviews*, 98, 171-200.

Davies, N. S., Gibling, M. R., & Rygel, M. C. (2011). Alluvial facies evolution during the Palaeozoic greening of the continents: case studies, conceptual models and modern analogues. *Sedimentology*, *58*, 220-258.

Davies, N.S., Gibling, M.R., McMahon, W.J., Slater, B.J., Long, D.G.F., Bashforth, A.R., Berry, C.M., Falcon-Lang, H.J., Gupta, S., Rygel, M.C., & Wellman, C.H. (2017a), Discussion on 'Tectonic and environmental controls on Palaeozoic fluvial environments: reassessing the impacts of early land plants on sedimentation'. Journal of the Geological Society,

https://doi.org/10.1144/jgs2016-063. Journal of the Geological Society, first published online [month] [date], [year], https://doi.org/10.1144/JGS2017-004

Davies, N. S., Liu, A. G., Gibling, M. R., & Miller, R. F. (2016) Resolving MISS conceptions and misconceptions: A geological approach to sedimentary surface textures generated by microbial and abiotic processes. *Earth-Science Reviews*, 154, 210-246.

Davies, N.S., Shillito, A.P., McMahon, W.J. (2017b). Short-term evolution of primary sedimentary surface textures (microbial, ichnological) on a dry stream bed: modern observations and ancient implications. *Palaios*, 32, 125-134.

de Almeida, R. P., Marconato, A., Freitas, B. T., & Turra, B. B. (2016). The ancestors of meandering rivers. *Geology*, *44*(3), 203-206.

De Boer, P. D. (1981). Mechanical effects of micro-organisms on intertidal bedform migration. *Sedimentology*, *28*(1), 129-132.

Endo, R. (1933) Manchuriophycus nov. gen., from a Sinian formation of South Manchuria. *Japanese Jour. Geol. Geogr*, 11, 1-2.

Eriksson, P. G. (2007). Classification of structures left by microbial mats in their host sediments. In *Atlas of microbial mat features preserved within the siliciclastic rock record* (p. 39).

Fedo, C. M., & Cooper, J. D. (1990) Braided fluvial to marine transition: the basal Lower Cambrian Wood Canyon Formation, southern Marble Mountains, Mojave Desert, California. *Journal of Sedimentary Research*, 60.

Field, J. (2001). Channel avulsion on alluvial fans in southern Arizona. *Geomorphology*, *37*(1), 93-104.

Fielding, C. R. (2006) Upper flow regime sheets, lenses and scour fills: extending the range of architectural elements for fluvial sediment bodies. *Sedimentary Geology*, 190, 227-240.

764 Fralick, P. (1999) Paleohydraulics of chute-and-pool structures in a Paleoproterozoic fluvial
765 sandstone. *Sedimentary Geology*, 125, 129-134.

766 Friend, P.F. (1983), Towards the field classification of alluvial architecture or sequence, in
767 Collinson, J.D., and Lewin, J., eds., Modern and Ancient Fluvial Systems: International Association
768 of Sedimentologists, Special Publication 6, p. 345–354.
769 Friend, P.F., Slater, M.J., AND Williams, R.C., 1979, Vertical and lateral building of river sandstone
770 bodies, Ebro Basin, Spain: Geological Society of London, Journal, v. 136, p. 39–46.
771 Fryberger, S. G., Schenk, C. J., & Krystinik, L. F. (1988) Stokes surfaces and the effects of near-
772 surface groundwater-table on Aeolian deposition. *Sedimentology*, 35, 21-41.
773 Fuller, A.O., 1985 A contribution to the conceptual modelling of pre-Devonian fluvial
774 systems. *Transactions Geological Society of South Africa* 88, 189–194.

775 Gibling, M. R., Davies, N. S., Falcon-Lang, H. J., Bashforth, A. R., DiMichele, W. A., Rygel, M. C., &
776 Ielpi, A. (2014) Palaeozoic co-evolution of rivers and vegetation: a synthesis of current
777 knowledge. *Proceedings of the Geologists' Association*, 125, 524-533.

778 Glumac, B., Curran, H. A., Motti, S. A., Weigner, M. M., & Pruss, S. B. (2011) Polygonal sandcracks:
779 Unique sedimentary desiccation structures in Bahamian ooid grainstone. *Geology*, 39, 615-618.

780 Gouramanis, C., Webb, J. A., & Warren, A. A. (2003) Fluviodeltaic sedimentology and ichnology of
781 part of the Silurian Grampians Group, western Victoria. *Australian Journal of Earth Sciences*, 50,
782 811-825.
783 Gracie, A. J., & Stewart, A. D. (1967) Torridonian sediments at Enard Bay, Ross-shire. *Scottish*
784 *Journal of Geology*, 3, 181-194.

785 Häntzschel,W., (1962) Trace fossils and Problematica. In: Moore, R.C. (Ed.), Treatise on
786 Paleontology (Part W, Conodonts, Conoidal Shells of Uncertain Affinities,Worms, Trace
787 Fossils, Problematica). Geological Society of America, Boulder, Colorado, and University
788 of Kansas, Lawrence. 177–245.

789 Holbrook, J., Scott, R. W., & Oboh-Ikuenobe, F. E. (2006). Base-level buffers and buttresses: a
790 model for upstream versus downstream control on fluvial geometry and architecture within
791 sequences. *Journal of Sedimentary Research*, *76*(1), 162-174.

792 Horton, A.J., Constantine, J.A., Hales, T.C., Goossens, B., Bruford, M.W., & Lazarus, E.D. (2017)
793 Modification of river meandering by tropical deforestation. *Geology*, doi:10.1130/G38740.1

794 Hunter, R. E. (1977) Basic types of stratification in small eolian dunes. *Sedimentology*, 24, 361-
795 387.

796 Hupp, C. R., & Osterkamp, W. R. (1996) Riparian vegetation and fluvial geomorphic processes.
797 *Geomorphology*, 14, 277-295.
798 Ielpi, A., & Ghinassi, M. (2015) Planview style and palaeodrainage of Torridonian channel belts:
799 Applecross Formation, Stoer Peninsula, Scotland. *Sedimentary Geology*, 325, 1-16.

800 Ielpi, A., & Rainbird, R. H. (2015). Architecture and morphodynamics of a 1· 6 Ga fluvial
801 sandstone: Ellice Formation of Elu Basin, Arctic Canada. *Sedimentology*, *62*(7), 1950-1977.
802 Ielpi, A., & Rainbird, R. H. (2016a) Highly Variable Precambrian Fluvial Style Recorded In the
803 Nelson Head Formation of Brock Inlier (Northwest Territories, Canada). *Journal of Sedimentary*
804 *Research*, 86, 199-216.

805 Ielpi, A., & Rainbird, R. H. (2016b) Reappraisal of Precambrian sheet-braided rivers: Evidence
806 for 1· 9 Ga deep-channelled drainage. *Sedimentology*.

807 Ielpi, A., Ventra, D., & Ghinassi, M. (2016) Deeply channelled Precambrian rivers: Remote
808 sensing and outcrop evidence from the 1.2 Ga Stoer Group of NW Scotland. *Precambrian*
809 *Research*.

810 Kennedy, J. F. (1963) The mechanics of dunes and antidunes in erodible-bed channels. *Journal of*
811 *Fluid Mechanics*, 16, 521-544.

812 Kinnaird, T. C., Prave, A. R., Kirkland, C. L., Horstwood, M., Parrish, R., & Batchelor, R. A. (2007)
813 The late Mesoproterozoic–early Neoproterozoic tectonostratigraphic evolution of NW Scotland:
814 the Torridonian revisited. *Journal of the Geological Society*, 164, 541-551.
815 Kocurek, G. (1981) Significance of interdune deposits and bounding surfaces in aeolian dune
816 sands. *Sedimentology*, 28, 753-780.
817 Kocurek, G. (1996) Desert aeolian systems.
818 Kocurek, G., & Fielder, G. (1982) Adhesion structures. *Journal of Sedimentary Research*, 52(4).
819 Kocurek, G., & Havholm, K. G. (1993) Eolian sequence stratigraphy-a conceptual framework.
820 Memoirs-American Association of Petroleum Geologists, 393-393.
821 Kocurek, G., & Nielson, J. (1986). Conditions favourable for the formation of warm-
822 climate aeolian sand sheets. *Sedimentology*, *33*(6), 795-816.
823 Koehn, D., Bons, P., Montenari, M., & Seilacher, A. (2014) The elastic age: rise and fall of
824 Precambrian biomat communities. In *EGU General Assembly Conference Abstracts* (Vol. 16, p.
825 13793).
826 Kovalchuk, O., Owttrim, G. W., Konhauser, K. O., & Gingras, M. K. (2017). Desiccation cracks in
827 siliciclastic deposits: Microbial mat-related compared to abiotic sedimentary origin.
828 *Sedimentary Geology*, *347*, 67-78.
829 Krabbendam, M. (2012) Stoer Group at Enard Bay. In Goodenough, K.M. & Krabbendam, M.
830 (eds.) A Geological Excursion Guide to the North-West Highlands of Scotland. Edinburgh
831 Geological Society, Edinburgh, pp. 74-84.
832 Krynine, P. D. (1948) The megascopic study and field classification of sedimentary rocks:
833 Journal of Geology, v. 56, p. 130–165.
834 Lancaster, N., & Baas, A. (1998) Influence of vegetation cover on sand transport by wind: field
835 studies at Owens Lake, California. *Earth Surface Processes and Landforms*, 23, 69-82.
836 Langford, R. P. (1989). Fluvial-aeolian interactions: Part I, modern systems. *Sedimentology*,
837 *36*(6), 1023-1035.

838 Long, D. G. (2006). Architecture of pre-vegetation sandy-braided perennial and ephemeral river
839 deposits in the Paleoproterozoic Athabasca Group, northern Saskatchewan, Canada as
840 indicators of Precambrian fluvial style. *Sedimentary Geology*, *190*(1), 71-95.

841 Lowe, D. G., & Arnott, R. W. C. (2016) Composition and Architecture of Braided and Sheetflood-
842 Dominated Ephemeral Fluvial Strata In the Cambrian–Ordovician Potsdam Group: A Case
843 Example of the Morphodynamics of Early Phanerozoic Fluvial Systems and Climate Change.
844 *Journal of Sedimentary Research*, 86, 587-612.

845 MacCulloch, J. (1819) A description of the western islands of Scotland, including the Isle of Man,
846 comprising an account of their geological structures, with remarks on their agriculture, scenery
847 and antiques. Constable, London, 3 Vols.

848 Marconato, A., de Almeida, R. P., Turra, B. B., & dos Santos Fragoso-Cesar, A. R. (2014) Pre-
849 vegetation fluvial floodplains and channel-belts in the Late Neoproterozoic–Cambrian Santa
850 Bárbara group (Southern Brazil). *Sedimentary Geology*, 300, 49-61.
851 McKee, E. D., Crosby, E. T., & Berryhill Jr, H. L. (1967). Flood deposits, Bijou Creek, Colorado, June
852 1965. *Journal of Sedimentary Research*, 37.
853 McMahon, S., van Smeerdijk Hood, A., & McIlroy, D. (2016). The origin and occurrence of
854 subaqueous sedimentary cracks. *Geological Society, London, Special Publications*, *448*, SP448-15.
855 McMahon, W. J., Davies, N. S., & Went, D. J. (2017). Negligible microbial matground influence on
856 pre-vegetation river functioning: Evidence from the Ediacaran-Lower Cambrian Series Rouge,
857 France. *Precambrian Research*, *292*, 13-34.

858 McManus, J., & Bajabaa, S. (1998). The importance of air escape processes in the formation of
859 dish-and-pillar and teepee structures within modern and Precambrian fluvial deposits.
860 *Sedimentary geology*, 120, 337-343.

861 Miall, A. D. (1985). Architectural-element analysis: a new method of facies analysis applied to
862 fluvial deposits. *Earth-Science Reviews*, *22*(4), 261-308.

Miall, A. D. (2014). *Fluvial depositional systems* (Vol. 14). Berlin: Springer.

Minter, N. J., Buatois, L. A., & Mángano, M. G. (2016). The conceptual and methodological tools of ichnology. In *The Trace-Fossil Record of Major Evolutionary Events* (pp. 1-26). Springer Netherlands.

Moor, H., Rydin, H., Hylander, K., Nilsson, M. B., Lindborg, R., & Norberg, J. (2017). Towards a trait-based ecology of wetland vegetation. *Journal of Ecology*.

Mountney, N. P. (2004). Feature: The sedimentary signature of deserts and their response to environmental change. *Geology Today*, 20, 101-106.

Mountney, N. P. (2012). A stratigraphic model to account for complexity in aeolian dune and interdune successions. *Sedimentology*, 59, 964-989.

Nicholson, P.G., (1993) A basin reappraisal of the Proterozoic Torridon Group, northwest Scotland. In: Frostick, L., Steel, R.J. (Eds.), Tectonic Controls and Signatures in Sedimentary Successions. *Special Publications of the International Association of Sedimentologists*, 20, 183–202.

Noffke, N., Gerdes, G., Klenke, T., & Krumbein, W. E. (2001) Microbially Induced Sedimentary Structures--A New Category within the Classification of Primary Sedimentary Structures: Perspectives. *Journal of Sedimentary Research*, 71, 649-656.

North, C. P., & Davidson, S. K. (2012). Unconfined alluvial flow processes: recognition and interpretation of their deposits, and the significance for palaeogeographic reconstruction. *Earth-Science Reviews*, *111*, 199-223.

Owen, G. (1995) Soft-sediment deformation in upper Proterozoic Torridonian sandstones (Applecross Formation) at Torridon, northwest Scotland. *Journal of Sedimentary Research*, 65.

Owen, G., Santos, M.G.M., (2014) Soft-sediment deformation in a pre-vegetation river system: the Neoproterozoic Torridonian of NW Scotland. *Proceedings of the Geologists' Association*, 125, 511–523.

888 Paola, C. H. R. I. S., Wiele, S. M., & Reinhart, M. A. (1989) Upper-regime parallel lamination as the
889 result of turbulent sediment transport and low-amplitude bed forms. *Sedimentology*, 36, 47-59.
890 Park, R. G., Stewart, A. D., & Wright, D. T. (2002). The Hebridean terrane. *The Geology of Scotland.*
891 *Geological Society, London*, 45-80.
892 Parnell, J., Mark, D., Fallick, A.E., Boyce, A., Thackrey, S., (2011) The age of the Mesoproterozoic
893 Stoer Group sedimentary and impact deposits, NWScotland. *Journal of the Geological Society,*
894 *London*, 168, 349–358.
895 Peach, B.N., Horne, J., Gunn,W., Clough, C.T., Hinxman, L.W., Teall, J.J.H., (1907) The geological
896 structure of the northwest highlands of Scotland. *Memoirs of the Geological Survey of Scotland.*
897 Prave, A. R. (2002) Life on land in the Proterozoic: Evidence from the Torridonian rocks of
898 northwest Scotland. *Geology*, 30, 811-814.
899 Rainbird, R. H. (1992). Anatomy of a large-scale braid-plain quartzarenite from the
900 Neoproterozoic Shaler Group, Victoria Island, Northwest Territories, Canada. *Canadian Journal*
901 *of Earth Sciences*, *29*(12), 2537-2550.
902 Rainbird, R., Cawood, P., & Gehrels, G. (2012) The great Grenvillian sedimentation episode:
903 Record of supercontinent Rodinia's assembly. *Tectonics of Sedimentary Basins: Recent Advances:*
904 *Blackwell Publishing Ltd*, 583-601.
905 Reid, I. & Frostick, L.E. (1994) Fluvial sediment transport and deposition. In *Sediment Transport*
906 *and Depositional Processes* (ed Pye K). Blackwell Scientific Publications, Oxford, pp. 89-156.
907 Reesink, A. J. H., Van den Berg, J. H., Parsons, D. R., Amsler, M. L., Best, J. L., Hardy, R. J., Orfea. O &
908 Szupiany, R. N. (2015) Extremes in dune preservation: Controls on the completeness of fluvial
909 deposits. *Earth-Science Reviews*, 150, 652-665.
910 Santos, M. G., Almeida, R. P., Godinho, L. P., Marconato, A., & Mountney, N. P. (2014) Distinct
911 styles of fluvial deposition in a Cambrian rift basin. *Sedimentology*, 61, 881-914.
912

913 Santos, M. G., & Owen, G. (2016) Heterolithic meandering-channel deposits from the
914 Neoproterozoic of NW Scotland: Implications for palaeogeographic reconstructions of
915 Precambrian sedimentary environments. *Precambrian Research*, 272, 226-243.
916 Saunderson, H. C., & Lockett, F. P. (1983) Flume experiments on bedforms and structures at the
917 dune-plane bed transition. In *Modern and Ancient Fluvial Systems* (Vol. 6, pp. 49-58).
918 International Association of Sedimentologists.
919 Schumm, S.A. (1968) Speculations concerning paleohydraulic controls of terrestrial
920 sedimentation. Geological Society of America Bulletin, 79, 1573–1588.
921 Schieber, J. (1999) Microbial mats in terrigenous clastics: the challenge of identification in the
922 rock record. Palaios, 14, 3–13.
923 Schieber J. (2007) Ripple patches in the Cretaceous Dakota Sandstone near Denver, Colorado, a
924 classic locality for microbially bound tidal sand flats. In Atlas of Microbial Mat Features
925 Preserved Within the Siliciclastic Rock Record (eds Schieber J, Bose PK, Eriksson PG, Banerjee S,
926 Sarkar S, Altermann W, Catuneanu O). Atlases in Geosciences. Elsevier, Amsterdam, pp. 222–
927 225.
928 Sedgwick, A., Muchison R.I. (1835). On the structure and the relations of the deposits
929 constrained between the Primary rocks and the Oolitic Series in the north of Scotland.
930 *Transactions of the Geological Society of London,* 2nd series, 3, 125 - 160
931 Selley, R. C. (1965) Diagnostic characters of fluviatile sediments of the Torridonian formation
932 (Precambrian) of northwest Scotland. *Journal of Sedimentary Research*, 35.
933 Shepard, R.N., Sumner, D.Y., (2010) Undirected motility of filamentous cyanobacteria produces
934 reticulate mats. *Geobiology*, 8, 179–190.
935 Simms, M. J. (2015) The Stac Fada impact ejecta deposit and the Lairg Gravity Low: evidence for
936 a buried Precambrian impact crater in Scotland?. *Proceedings of the Geologists' Association*, 126,
937 742-761.
938 Smith, R. L., Stearn, J. E. F., & Piper, J. D. A. (1983) Palaeomagnetic studies of the Torridonian
939 sediments, NW Scotland. *Scottish Journal of Geology*, 19(1), 29-45.

940 Stein, A. M. (1988) Basement controls upon basin development in the Caledonian foreland, NW
941 Scotland. *Basin Research*, 1, 107-119.
942 Stein, A. M. (1992) Basin development and petroleum potential in The Minches and Sea of the
943 Hebrides Basins. *Geological Society, London, Special Publications*, 62, 17-20.
944 Stewart, A.D., (1969). Torridonian rocks of Scotland reviewed. In: Kay, M. (Ed.), North
945 Atlantic—Geology and Continental Drift: A Symposium. *American Association of Petroleum*
946 *Geologists Memoir*, 12, 595–608.
947 Stewart, A.D., (1982). Late Proterozoic rifting in NW Scotland: the genesis of the
948 'Torridonian'. Journal of the Geological Society, London, 139, 413–420.
949 Stewart, A. D. (1990). Geochemistry, provenance and climate of the Upper Proterozoic Stoer
950 Group in Scotland. *Scottish Journal of Geology*, *26*(2), 89-97.
951
952 Stewart, A. D. (1991). Geochemistry, provenance and palaeoclimate of the Sleat and Torridon
953 groups in Skye. *Scottish Journal of Geology*, 27, 81-95.
954 Stewart, A.D., (2002). The later Proterozoic Torridonian rocks of Scotland: their sedimentology,
955 geochemistry, and origin. *Geological Society, London, Memoir*, 24.
956 Stewart, A.D., Donnellan, N.C.B., (1992). Geochemistry and provenance of red sandstones in the
957 Upper Proterozoic Torridon Group in Scotland. Scottish Journal of Geology 28,143–153.
958 Stewart and Irving, E (1974) Palaeomagnetism of Precambrian sedimentary rocks from north-
959 west Scotland and the apparent polar wander path of Laurentia. *Geophys. f. R. Astron. Soc.* 37, 57-
960 72.
961 Strother, P. K., & Wellman, C. H. (2016) Palaeoecology of a billion-year-old non-marine
962 cyanobacterium from the Torridon Group and Nonesuch Formation. *Palaeontology*, *59*(1), 89-
963 108.
964 Strother, P. K., Battison, L., Brasier, M. D., & Wellman, C. H. (2011) Earth/'s earliest non-marine
965 eukaryotes. *Nature*, 473, 505-509.
966 Teall, J.J.H. (1907) The Petrography of the Torridonian Formation. *Memoirs of the*

967 *Geological Survey of Great Britain*, 278–290.

968 Thorne, C.R. (1990) Effects of vegetation on Riverbank erosion and stability. In: Thornes,
969 J.W. (Ed.), Vegetation and Erosion: Processes and Environments. John Wiley and Sons,
970 Chichester, 125–144.
971 Tipper, J. C. (2015). The importance of doing nothing: stasis in sedimentation systems and its
972 stratigraphic effects. *Geological Society, London, Special Publications*, *404*(1), 105-122.
973 Tirsgaard, H., & Øxnevad, I. E. (1998) Preservation of pre-vegetational mixed fluvio–aeolian
974 deposits in a humid climatic setting: an example from the Middle Proterozoic Eriksfjord
975 Formation, Southwest Greenland. *Sedimentary Geology*, 120, 295-317.
976 Todd, S. P., & Went, D. J. (1991). Lateral migration of sand-bed rivers: examples from the
977 Devonian Glashabeg Formation, SW Ireland and the Cambrian Alderney Sandstone Formation,
978 Channel Islands. *Sedimentology*, *38*(6), 997-1020.
979 Torsvik, T. H., & Sturt, B. A. (1987). On the origin and stability of remanence and the magnetic
980 fabric of the Torridonian Red Beds, NW Scotland. *Scottish Journal of Geology*, *23*(1), 23-38.
981 Trewin, N. H. (1993) Controls on fluvial deposition in mixed fluvial and aeolian facies within the
982 Tumblagooda Sandstone (Late Silurian) of Western Australia. *Sedimentary Geology*, 85, 387-400.
983 Turnbull, M. J., Whitehouse, M. J., & Moorbath, S. (1996) New isotopic age determinations for the
984 Torridonian, NW Scotland. *Journal of the Geological Society*, 153, 955-964.
985 Van de Kamp, P. C., & Leake, B. E. (1997) Mineralogy, geochemistry, provenance and sodium
986 metasomatism of Torridonian rift basin clastic rocks, NW Scotland. *Scottish Journal of Geology*,
987 33, 105-124.
988 Van Mechelen, J. L. M. (2004). Strength of moist sand controlled by surface tension for tectonic
989 analogue modelling. *Tectonophysics*, *384*(1), 275-284.
990 Williams, G. E. (1966) The Precambrian Torridonian sediments of the Cape Wrath district,
991 north-west Scotland. *Univ. Reading Ph.D thesis,* (unpubl.).
992 Williams, G. E. (2001) Neoproterozoic (Torridonian) alluvial fan succession, northwest Scotland,
993 and its tectonic setting and provenance. *Geological Magazine*, 138, 161-184.

994 Williams, G. E., & Foden, J. (2011) A unifying model for the Torridon Group (early
995 Neoproterozoic), NW Scotland: Product of post-Grenvillian extensional collapse. *Earth-Science*
996 *Reviews*, 108, 34-49.
997 Williams, G. E., & Schmidt, P. W. (1997) Palaeomagnetic dating of sub-Torridon Group
998 weathering profiles, NW Scotland: verification of Neoproterozoic palaeosols. *Journal of the*
999 *Geological Society*, 154, 987-997.
1000 Winston, D. (2016) Sheetflood sedimentology of the Mesoproterozoic Revett Formation, Belt
1001 Supergroup, northwestern Montana, USA. *Geological Society of America Special Papers*, 522
1002 Young, G. M. (1999). Some aspects of the geochemistry, provenance and palaeoclimatology of
1003 the Torridonian of NW Scotland. *Journal of the Geological Society*, 156, 1097-1111.
1004
1005
1006
1007
1008
1009
1010
1011
1012
1013
1014
1015
1016

Figure 1. (A) Geological map of the informal Torridonian Supergroup; (B) Higher resolution maps of MDF locations of study; (C) Stratigraphic column of the stratigraphy of the NW Scottish Highlands.

Figure 2. Representative stratigraphic logs of Facies Associations 1 and 2. Sr = ripple marks.

Figure 3. (A) Planform surfaces at Rubha Réidh. The microtopography of the surface is dictated by the underlying lithofacies. If horizontal-laminations (Sh) comprise the topmost lithofacies of the underlying sand-body, topography is flat (B). If dune cross-stratification comprise the topmost lithofacies of the underlying sand-body, dune microtopography is preserved (C). Each planform surface is near ubiquitously covered in ripple marks.

Figure 4. Possible chute and pool structures at: (A) Rubha Réidh; (B) Stoer (inaccessible cliff exposure). Upstream-dipping bedding truncates against the steeper, down-flow dipping surfaces ('Pool'). Convex up bedding passes over topographic high ('Chute').

Figure 5. (A) Solitary antidune stratification, with backset cross-bedding dipping against prevailing palaeoflow; (B) Convex-up bedding possibly representative of antidune stratification. (Both images from Rubha Réidh)

Figure 6. Architectural panel of Meall Dearg outcrop (Rubha Réidh).

Figure 7. (A) Humpback cross-stratification at Rubha Réidh; (B) Three-dimensional exposures show the westward outbuilding of wedge-shaped humpback cross-stratified packages. Sh = horizontal-laminations; Sl = Low-angle cross-stratification; Sr = Ripple marks

Figure 8. (A) Low-angle cross-stratification at Balchladich Bay (Sl); (B) Alternating sets of horizontal-laminated (Sh) and planar cross-stratified (Sp) sandstones at Stoer.

Figure 9. (A) Ripple marks superimposed onto dune topography; (B) Planar surface with ripple marks

Figure 10. Morphology of preserved ripple-marks: (A) Drainage marks etched in flanks of ripple marks; (B) Sharp crested ripple crests; (C) Synaeresis cracks in ripple troughs; (D) Interference ripple marks; (E) Mud draped ripple marks within dune trough; (F) Ripple marks preserved in vertical section; (G) Oversteepened ripple marks; (H) Desiccated mudstones; (i) Desiccated polygons overprinting rippled sandstone, no mud preserved. All photos from Rubha Réidh.

1043 Figure 11. Schematic illustration and photographs of adhesion mark distribution across Meall Dearg
1044 fluvial facies.

1045 Figure 12. Examples of *Manchuriophycus* at Rubha Réidh. Fragments of possible '*Manchuriophycus*'
1046 highlighted in red.

1047 Figure 13. Possible microbial sedimentary surface textures at Rubha Réidh: (A, B) Reticulate markings
1048 preserved at Rubha Réidh; (C) Clear margin separating sandstone with and without adhesion marks.

1049 Figure 14. (A) Desiccated sandstone surface; (B) Desiccated mudstone surface. Both Rubha Réidh

1050 Figure 15. (A) Intercalated planar cross-stratified dunes and planar-bedded interdunes at Enard Bay.
1051 Person is 187 cm. Restored to horizontal; (B) Aeolian dune geometry in depositional-dip sections; (C)
1052 Aeolian dune geometry in depositional-strike sections; (D) Large scale arcuate aeolian dune-forms; (E)
1053 Palaeoflow dispersal across an individual aeolian dune-form. All Enard Bay.

1054 Figure 16. Exposure of occasionally pebbly, coarse-grained, cross-bedded sandstone apparently faulted
1055 into contact with the rest of the Meall Dearg Formation at Enard Bay

1056 Figure 17. Sedimentary structures at Enard Bay: (A) Cross laminae in dune facies (interpreted grainflow
1057 deposits). Restored to horizontal; (B) Textural and mineralogical character of dune facies as observed in
1058 thin-sectioned samples under polarized light (C) Planar laminations in dune facies (interpreted grainfall
1059 deposits); (D) Wind-ripple horizontal laminae define pin-stripe laminations; (E) Adhesion warts
1060 preserved on interdune surface; (F) Possible adhesion lamination in interdune facies. Photographs A – D
1061 are not restored to horizontal.

1062 Figure 18. (A) Dune sets separated by low-angle, erosional reactivation surfaces (dashed line). Person is
1063 187 cm; (B) Channel-body incising into 2.4 m thick planar-bedded package (Enard Bay).

1064 Figure 19. Limitations of Meall Dearg Formation coastal exposures for determining large-scale
1065 depositional architecture: (A) Tectonic dip (25-30°) renders the exposure unsuitable for interpretation
1066 from satellite imagery because surficial cross-sectional exposure of beds is oblique to land surface; (B)
1067 Coastal exposure disappears beneath a variably deep drift cover of post-glacial till and peat bog, making it

impossible to trace bedding for greater than 140 m. Photograph restored to horizontal. Meall Dearg outcrop highlighted in green in both photographs.

Fig. 1

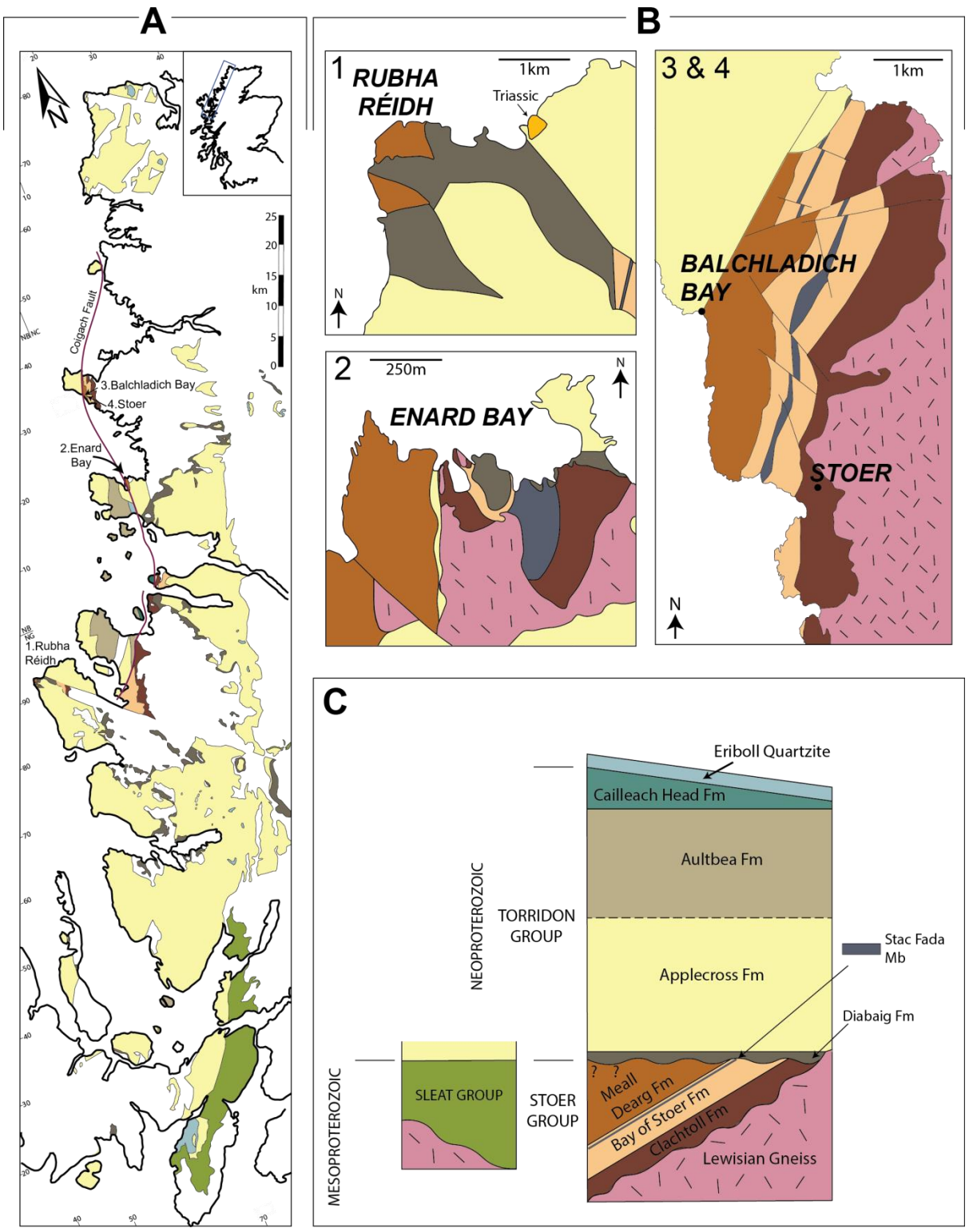
A
B
C
Colgach Fault
3.Balchladich Bay
4.Stoer
2.Enard Bay
1.Rubha Réidh
25
20
15
km
10
5
0
1
RUBHA RÉIDH
1km
Triassic
N
2
250m
ENARD BAY
3 & 4
1km
BALCHLADICH BAY
STOER
Eriboll Quartzite
Cailleach Head Fm
Aultbea Fm
TORRIDON GROUP
NEOPROTEROZOIC
Applecross Fm
Stac Fada Mb
Diabaig Fm
SLEAT GROUP
STOER GROUP
MESOPROTEROZOIC
Meall Dearg Fm
Bay of Stoer Fm
Clachtoll Fm
Lewisian Gneiss

Fig. 2

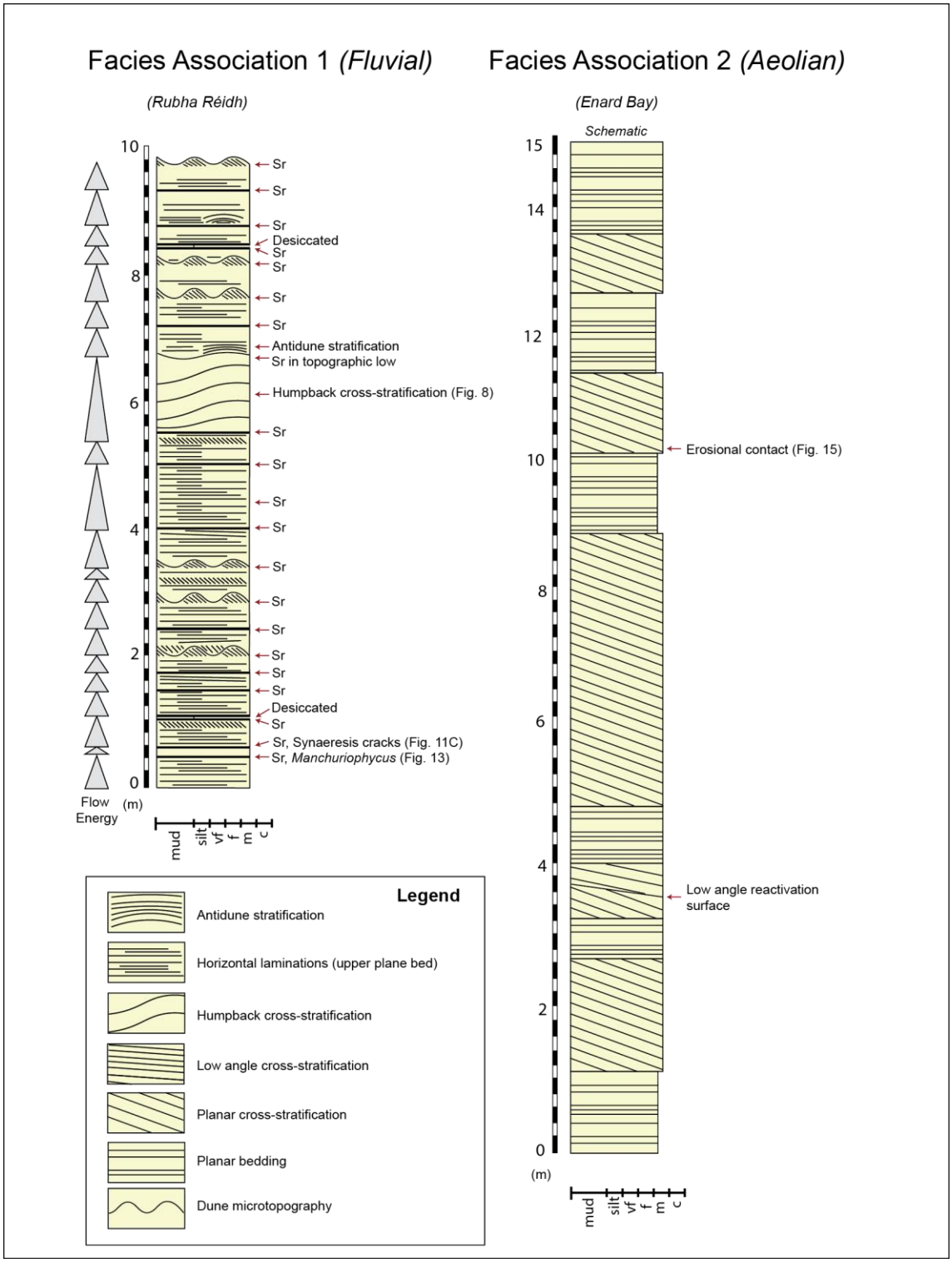
Facies Association 1 (Fluvial)
(Rubha Réidh)
Facies Association 2 (Aeolian)
(Enard Bay)
Schematic
Sr
Desiccated
Antidune stratification
Sr in topographic low
Humpback cross-stratification (Fig. 8)
Sr, Synaeresis cracks (Fig. 11C)
Sr, Manchuriophycus (Fig. 13)
Erosional contact (Fig. 15)
Low angle reactivation surface
Flow Energy
(m)
mud
silt
vf
f
m
c
Legend
Antidune stratification
Horizontal laminations (upper plane bed)
Humpback cross-stratification
Low angle cross-stratification
Planar cross-stratification
Planar bedding
Dune microtopography

Fig. 3

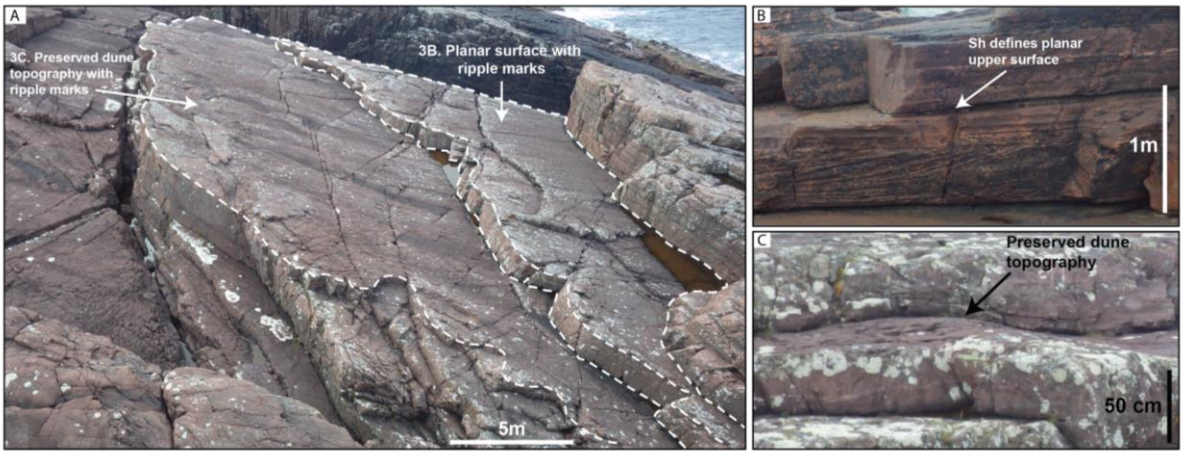
A
3C. Preserved dune topography with ripple marks
3B. Planar surface with ripple marks
5m
B
Sh defines planar upper surface
1m
C
Preserved dune topography
50 cm

Fig. 4

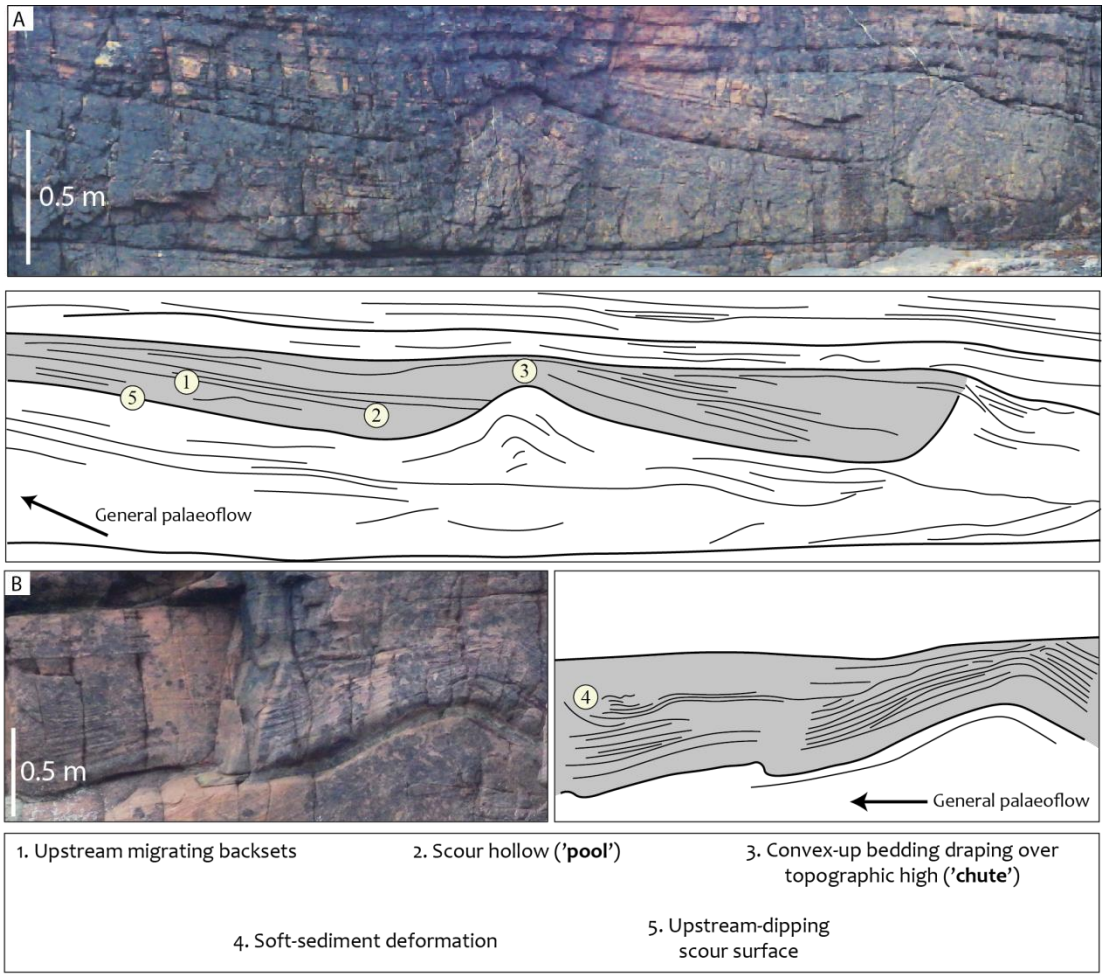
A
0.5 m
1
2
3
5
General palaeoflow
B
0.5 m
4
General palaeoflow
1. Upstream migrating backsets
2. Scour hollow ('pool')
3. Convex-up bedding draping over topographic high ('chute')
4. Soft-sediment deformation
5. Upstream-dipping scour surface

Fig. 5

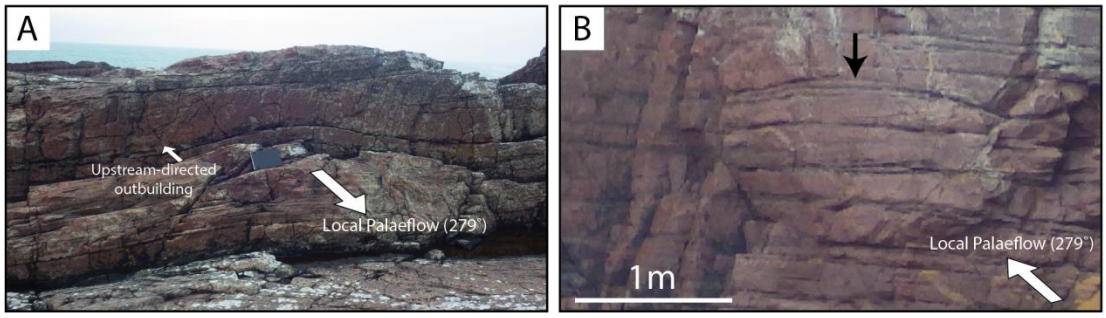

Fig. 6

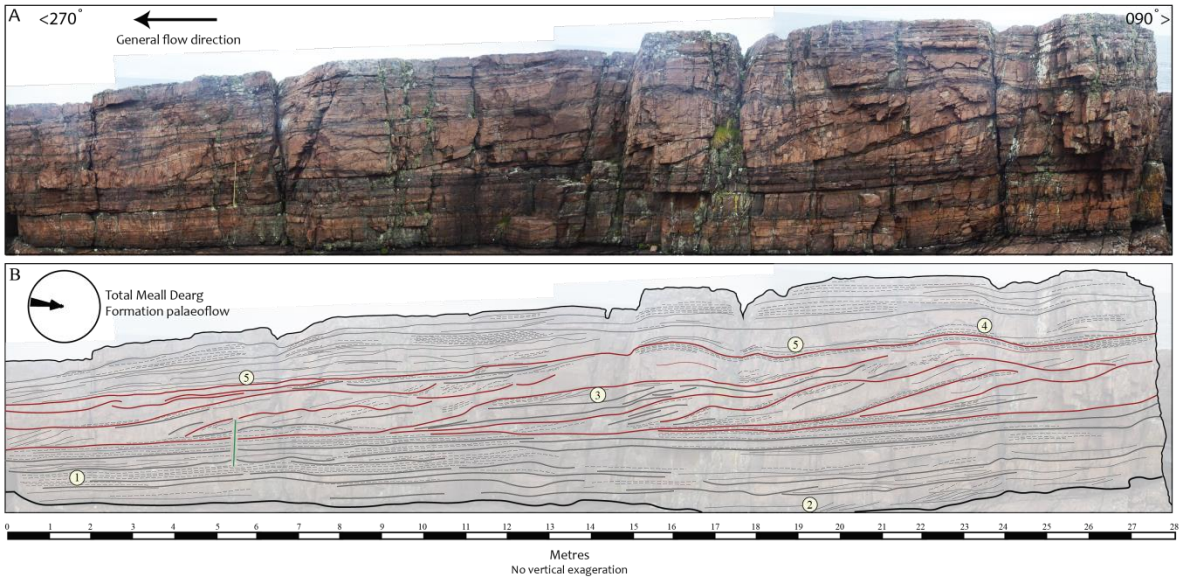

Fig. 6 (cont)

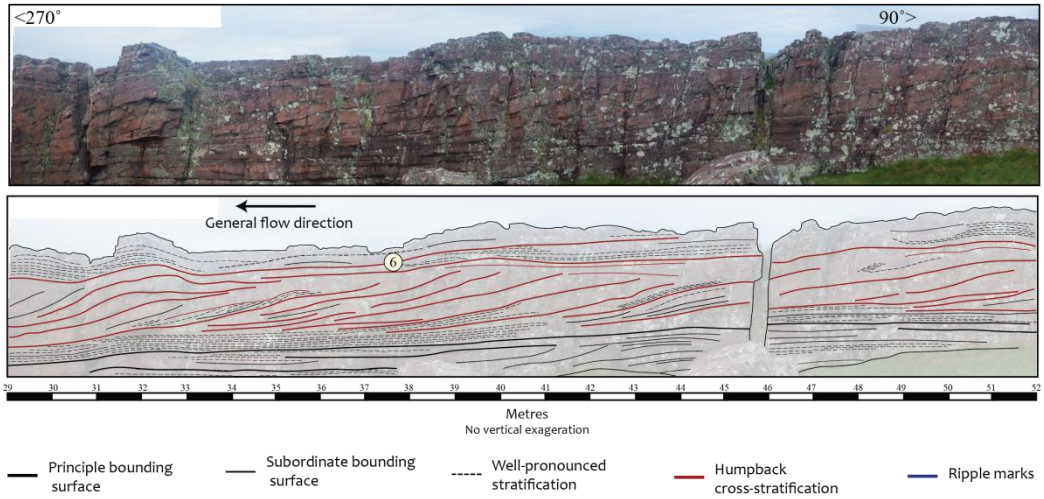

Fig. 6cont

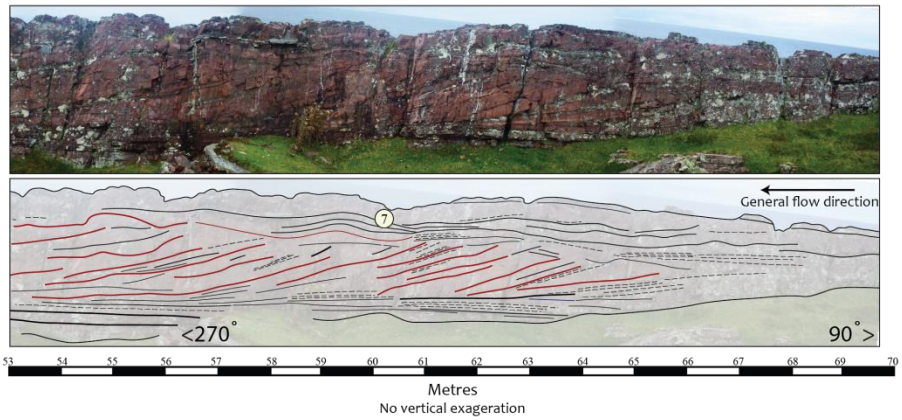

1. Sets of horizontal laminations orgnised within a tabular package. Bottom sets of internal packages dip gently down-flow

2. Lower flow regime cross-stratification are restricted to isolated sets and frequently have top surfaces eroded by horizontal laminations

3. Fig. 7: Humpback cross-stratification. Convex-up bed topography constitutes a form set which grades down-flow (west) into a relatively large foreset and in turn into an extensive, flat-laminated bottomset

4. Low relief, convex-upward, largely symmetrical bedding with backset cross-stratification are interpreted as antidune stratification

5. Above humpback cross-stratification, ripple marks are preserved in troughs only, where water would have pooled during waning flow conditions

6. Horizontal laminated package thins downstream and transitions into humpback cross-stratification

7. Convex-up, symmetrical antidune with backset cross-bedding evolving from underlying humpback cross-stratified package

Fig. 7

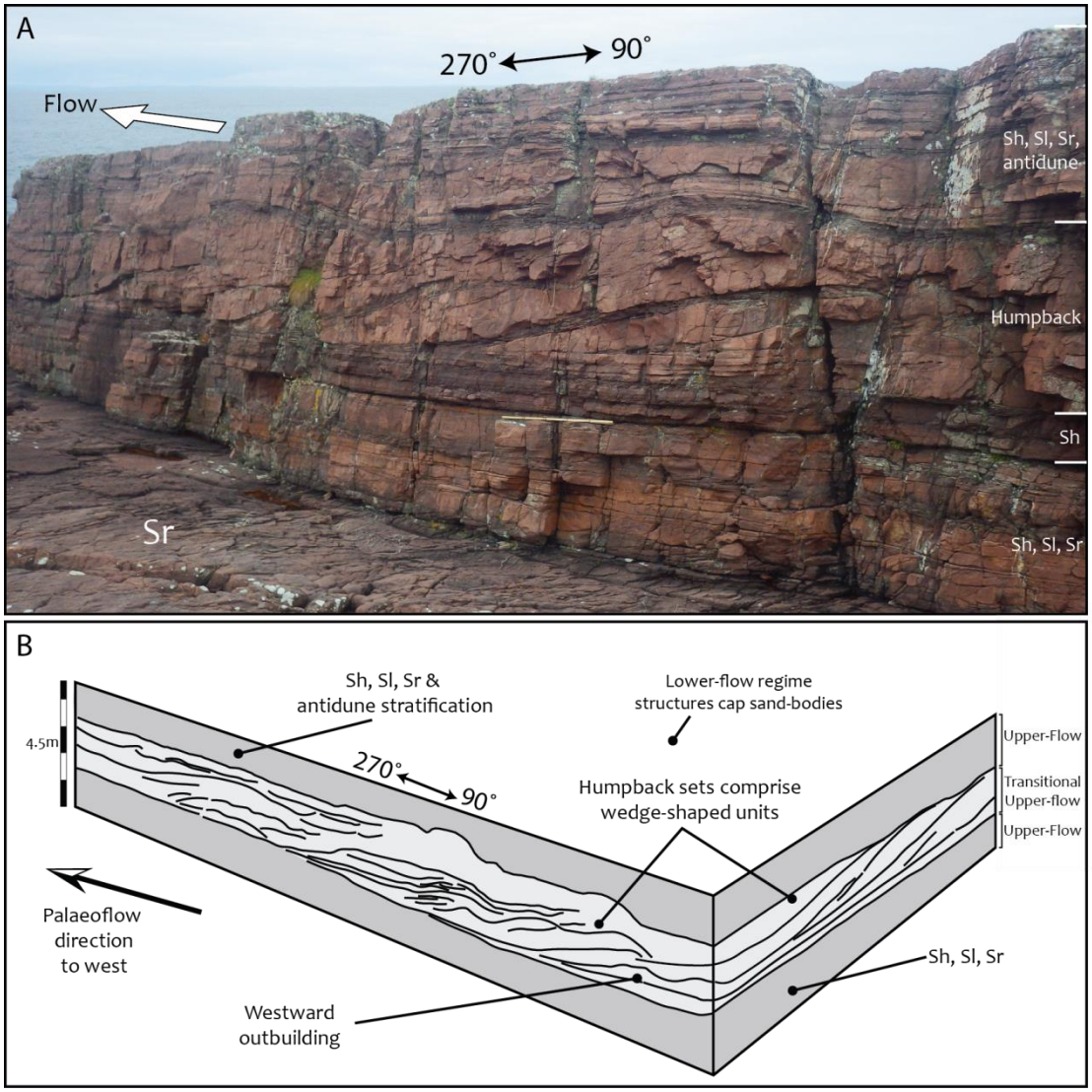
A
270°
90°
Flow
Sh, Sl, Sr,
antidune
Humpback
Sh
Sr
Sh, Sl, Sr
B
Sh, Sl, Sr &
antidune stratification
Lower-flow regime
structures cap sand-bodies
4.5m
270°
90°
Humpback sets comprise
wedge-shaped units
Upper-Flow
Transitional
Upper-flow
Upper-Flow
Palaeoflow
direction
to west
Sh, Sl, Sr
Westward
outbuilding

Fig. 8

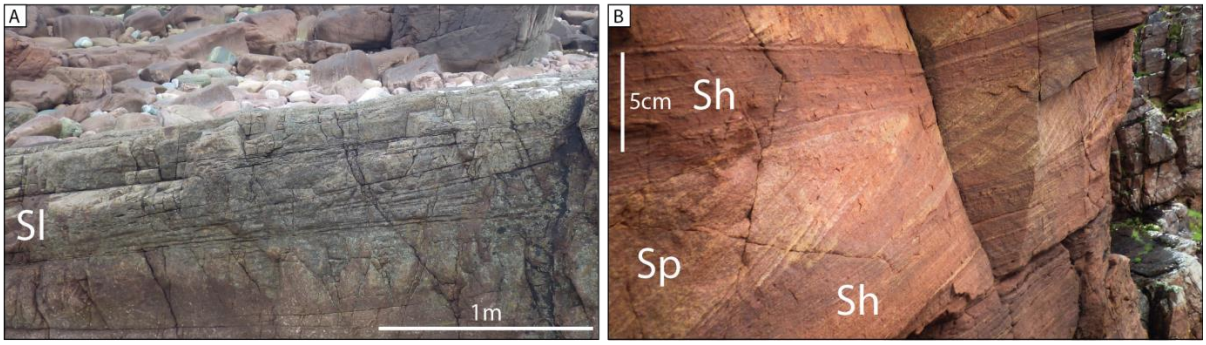
A
Sl
1m
B
5cm
Sh
Sp
Sh

Fig. 9

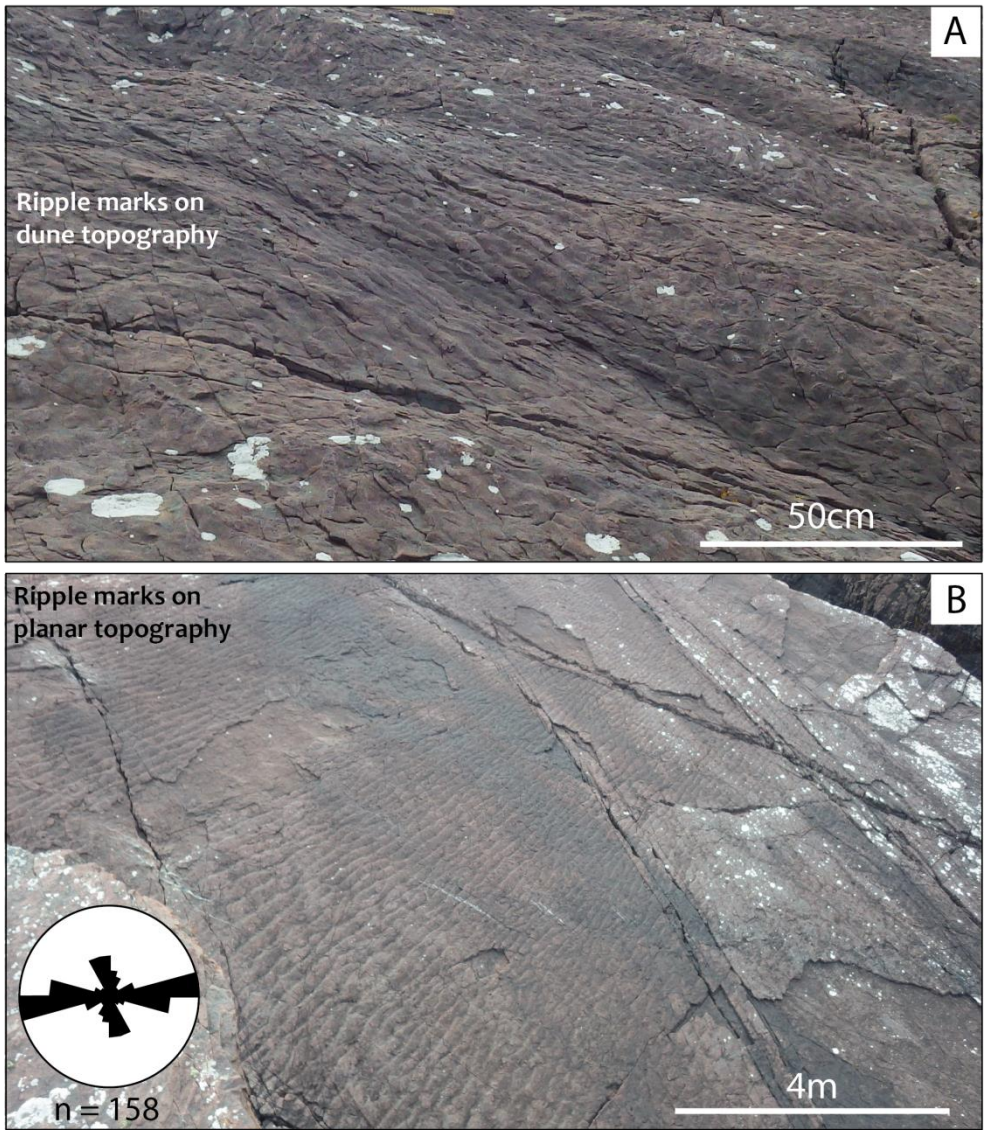
A
Ripple marks on
dune topography
50cm
B
Ripple marks on
planar topography
n = 158
4m

Fig. 10.

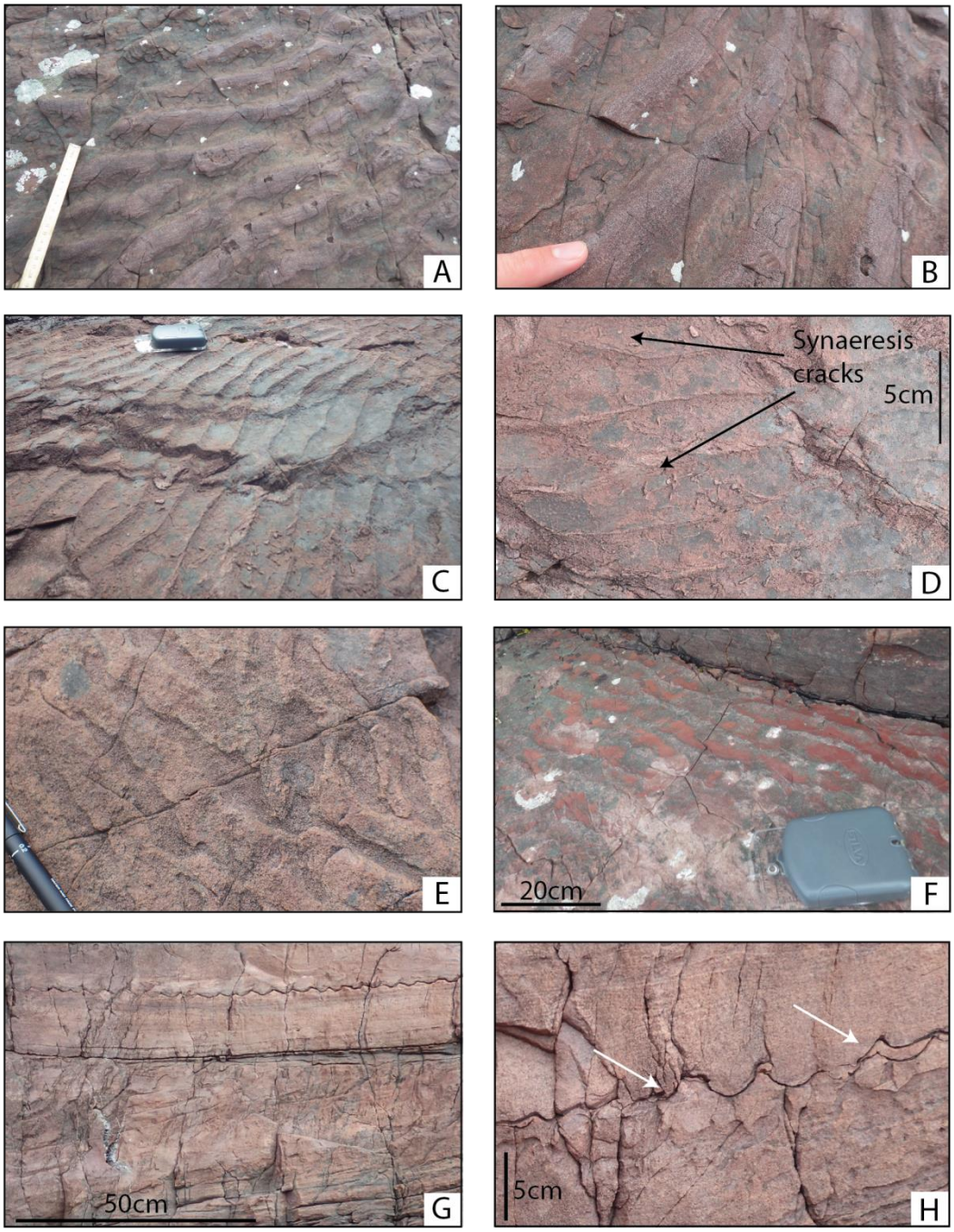

Fig. 11.

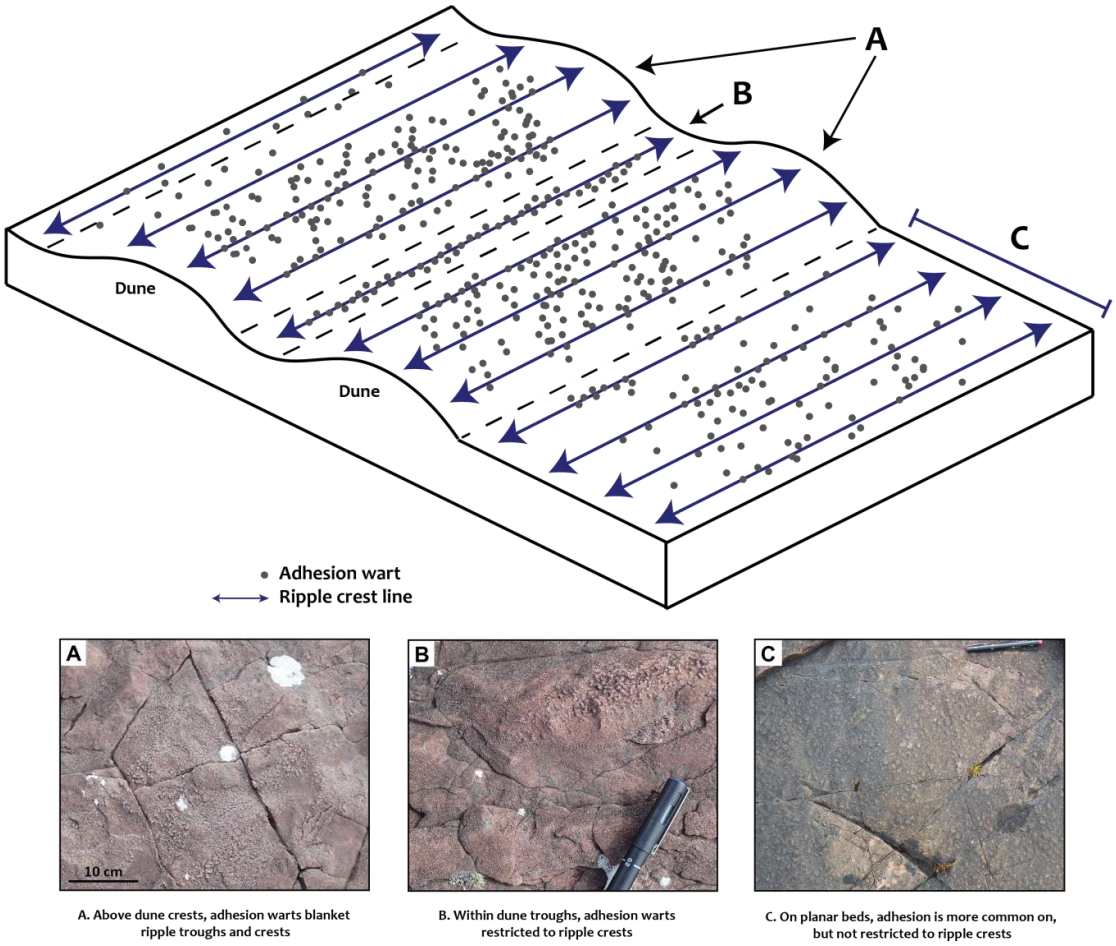

A. Above dune crests, adhesion warts blanket ripple troughs and crests

B. Within dune troughs, adhesion warts restricted to ripple crests

C. On planar beds, adhesion is more common on, but not restricted to ripple crests

Fig. 12

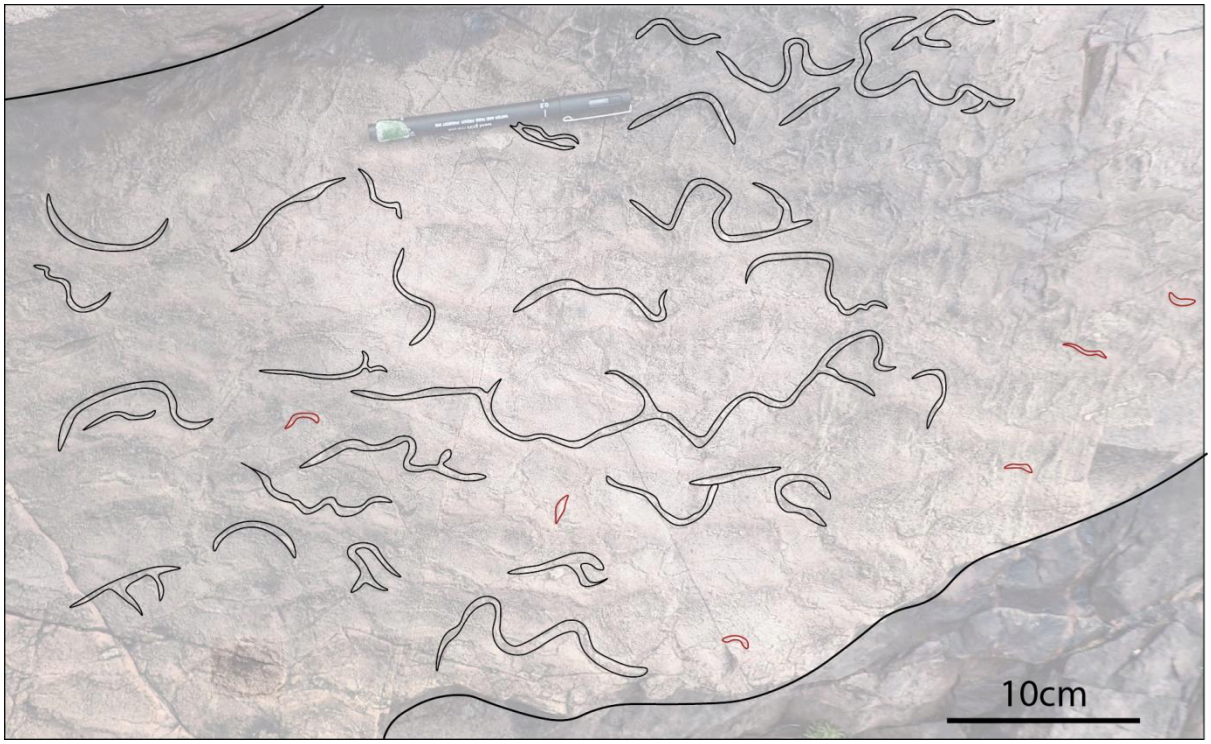

Fig. 13

77

78

79 Fig. 14

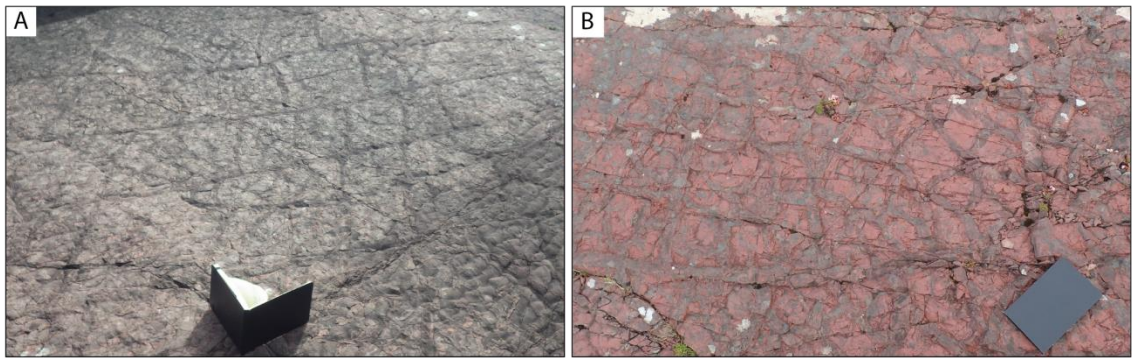

80

81 Fig. 15

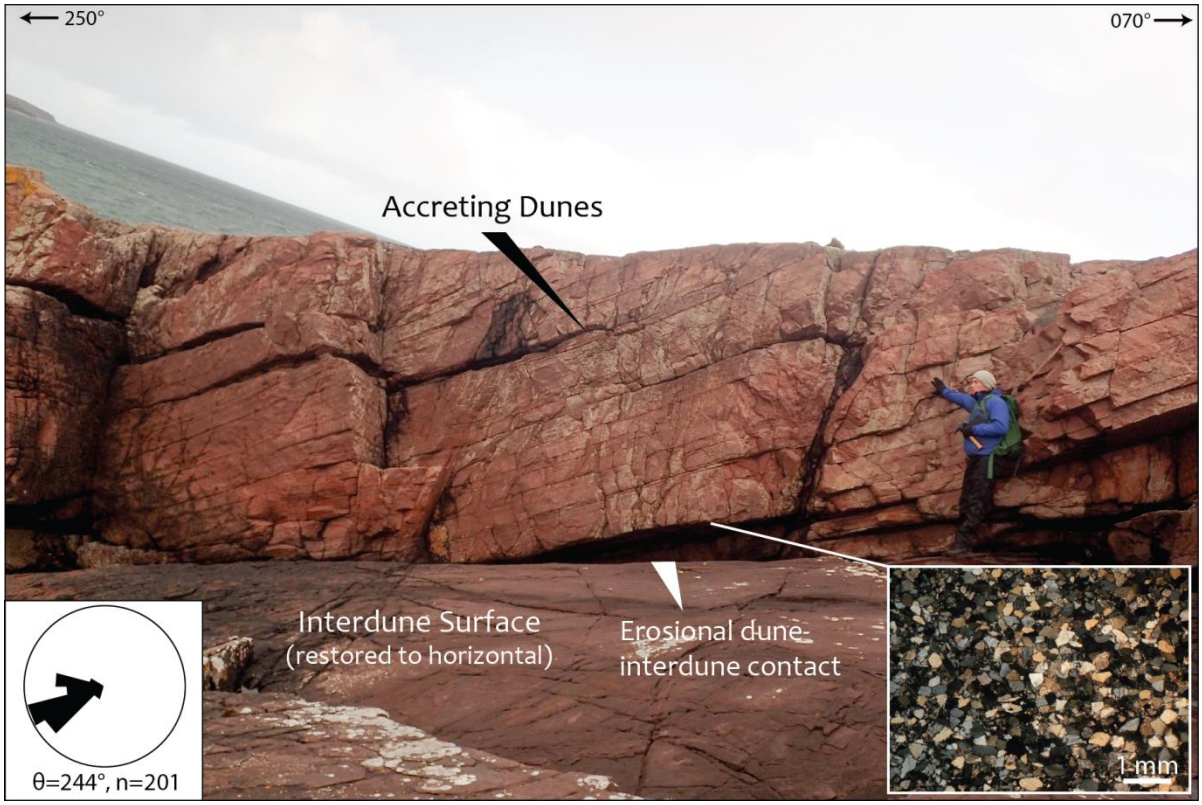
250°
070°
Accreting Dunes
Interdune Surface
(restored to horizontal)
Erosional dune-
interdune contact
θ=244°, n=201
1 mm

Fig.16

Fig. 16

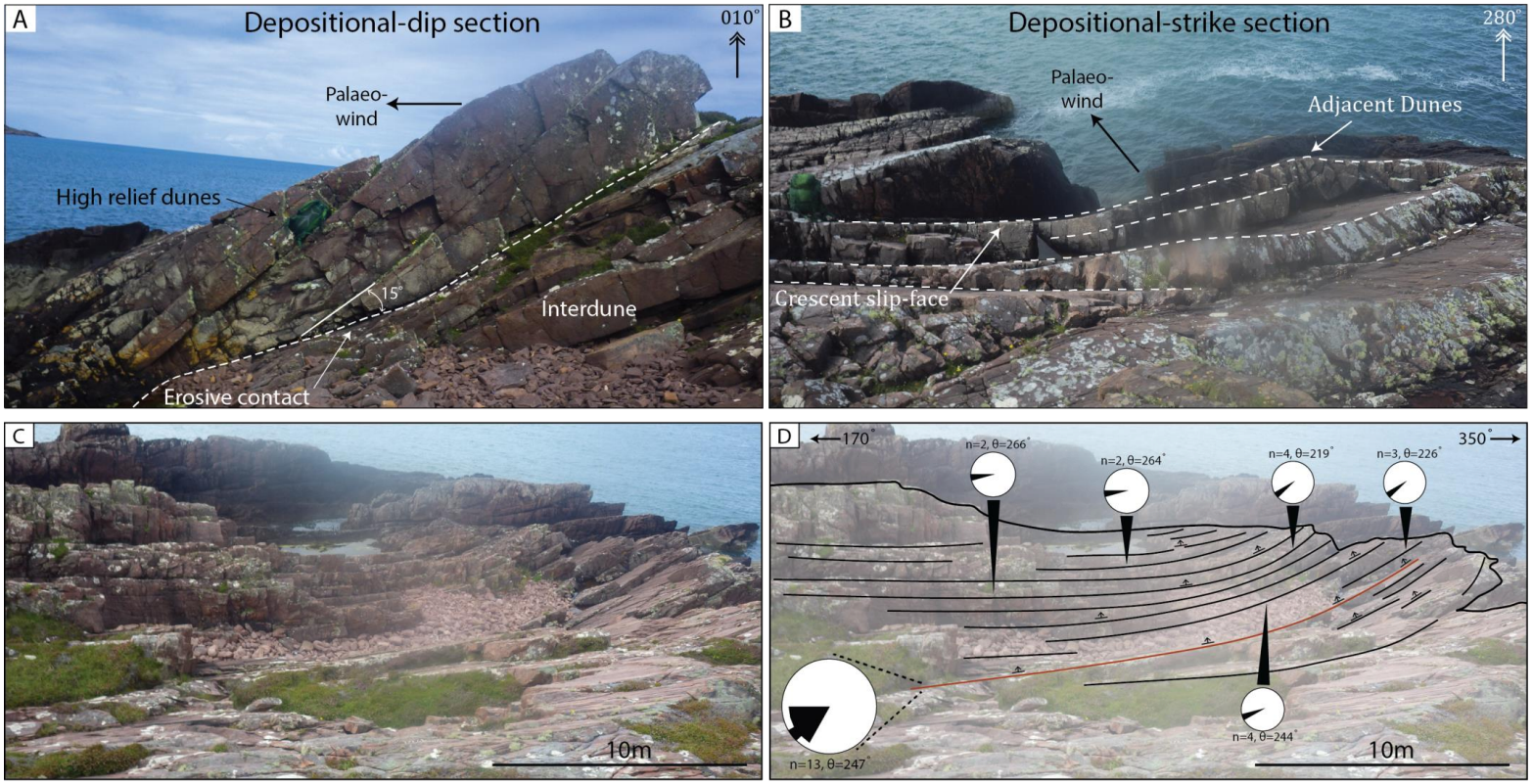
A
Depositional-dip section
010°
Palaeo-
wind
High relief dunes
15°
Interdune
Erosive contact
B
Depositional-strike section
280°
Palaeo-
wind
Adjacent Dunes
Crescent slip-face
C
10m
D
170°
350°
n=2, θ=266°
n=2, θ=264°
n=4, θ=219°
n=3, θ=226°
n=4, θ=244°
n=13, θ=247°
10m

Fig. 17


Continuous succession of
FA2 strata
Tectonic dip &
strike of beds
22
Singular outcrop of pebbly
coarse-grained sandstone
(see inset)
Tectonic dip &
strike of beds
32

Fig. 18

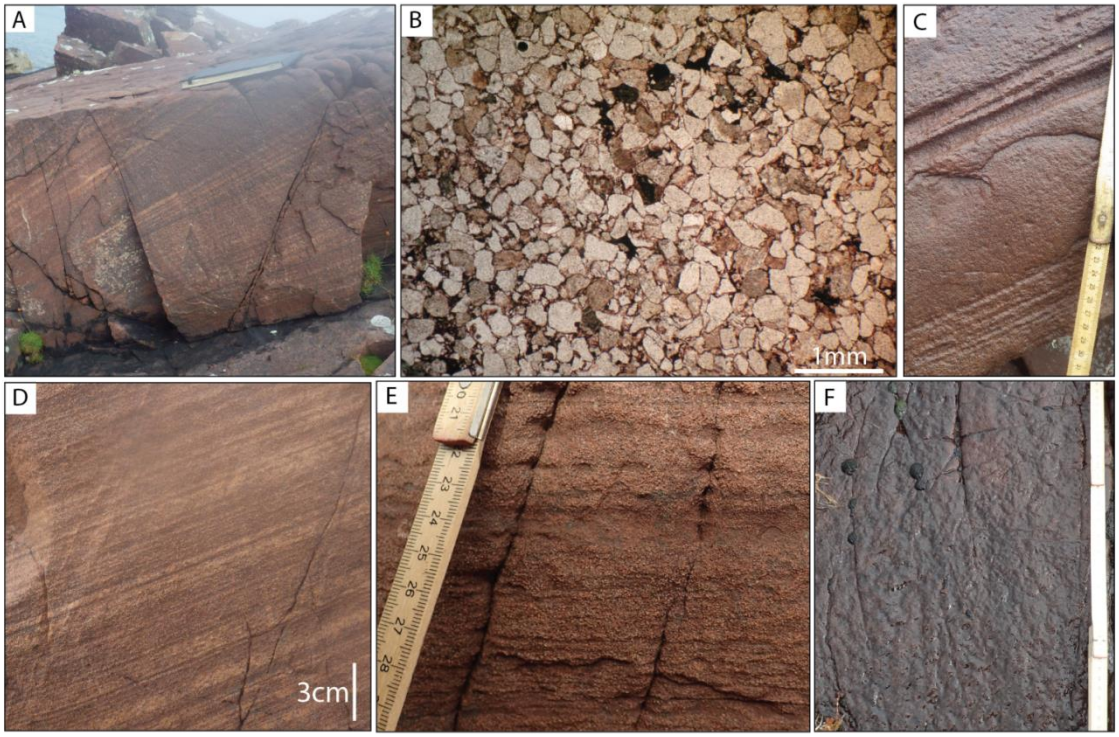

Fig. 19.


270°
1mm
Restored to horizontal

Fig. 20.

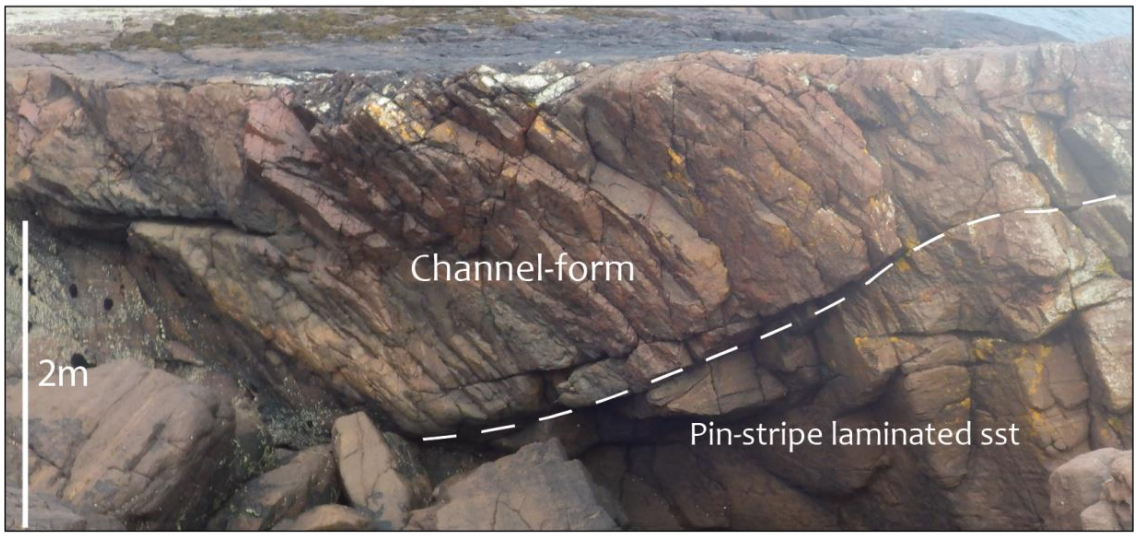
Channel-form
2m
Pin-stripe laminated sst

120 Fig. 21.

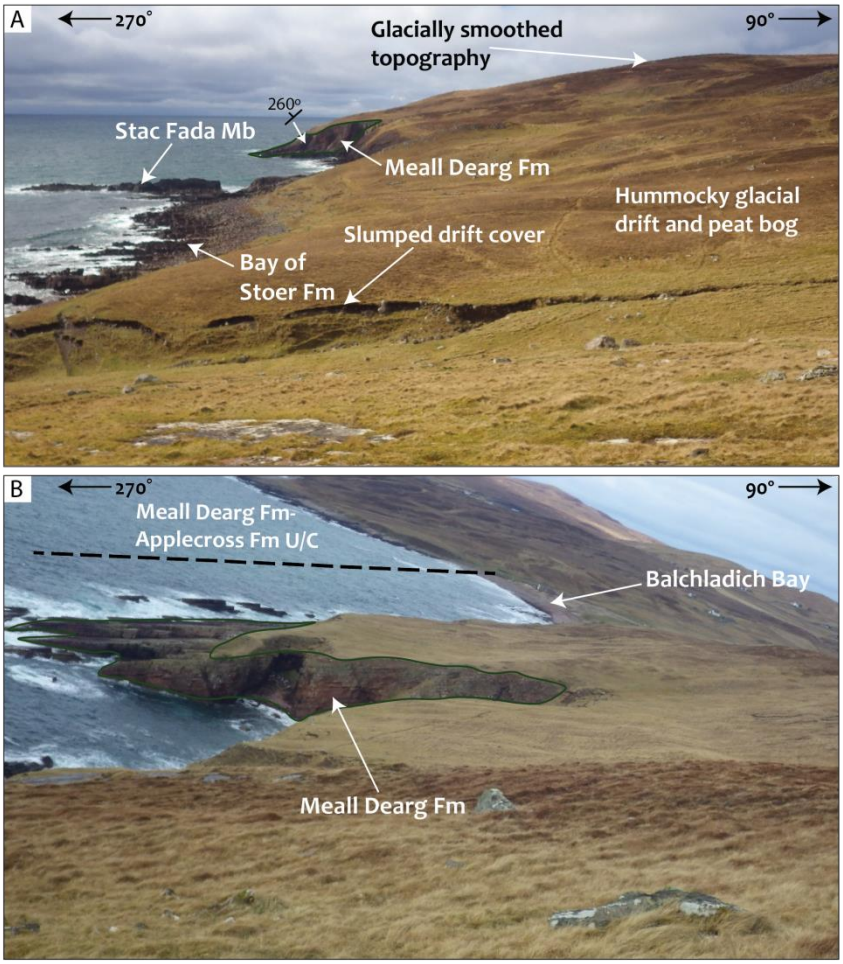

121

122

Table 1. Distribution of sedimentary structures across Meall Dearg locations. See text for information regarding frequency of occurrence.

Facies Association	Location	Type of exposure	Horizontal laminations	Antidune Stratification	Chute and Pool Structures	Humpback cross-stratification	Low angle cross-stratification	Planar cross-stratification	Trough cross-stratification	Ripple-marks	Adhesion marks	*Manchurio-phycus*	Reticulate marks	Planar Bedding
FA1	Stoer	Vertical cliffs	Y		Y		Y	Y	Y	Y	Y			
	Rubha Réidh	Stepped wave-cut platforms	Y	Y	Y	Y	Y	Y		Y	Y	Y	Y	
	Bachladich Bay	Stepped wave-cut platforms	Y	Y			Y	Y		Y	Y			
FA2	Enard Bay	Stepped wave-cut platforms						Y		Y				Y